GENERALIZING DYNAMICS MODELING EASIER FROM REPRESENTATION PERSPECTIVE

Anonymous authors
Paper under double-blind review

ABSTRACT

Learning system dynamics from observations is a critical problem in many applications over various real-world complex systems, *e.g.,* climate, ecology, and fluid systems. Recently, the neural-based dynamics modeling method has become the prevalent solution, where its basic idea is to embed the original states of objects into a latent space before learning the dynamics using neural-based methods such as neural Ordinary Differential Equations (ODE). Given observations from different complex systems, the existing dynamics modeling methods offer a specific model for each observation, resulting in poor generalization. Inspired by the great success of pre-trained models, we raise a question: whether we can conduct a generalized **P**re-trained **D**ynamic **E**nco**DER** (**PDEDER**), which, for various complex systems, can embed their original states into a latent space, where the dynamics can be easier captured. To conduct this generalized PDEDER, we collect 153 sets of real-world and synthetic observations from 24 complex systems. Inspired by the success of time series forecasting using Pre-trained Language Models (PLM), we can employ any PLM and further update it over these dynamic observations by tokenization techniques to achieve the generalized PDEDER. Given any future dynamic observation, we can fine-tune PDEDER with any specific dynamics modeling method. We evaluate PDEDER on 18 dynamic systems by long/short-term forecasting under both in-domain and cross-domain settings and the empirical results indicate the effectiveness of PDEDER.

1 INTRODUCTION

System dynamics, which describes the object states evolving over time, is a powerful methodology to conceptualize complex systems from various domains, *e.g.,* climate, ecology, and fluid systems (Alon, 2006; Bashan et al., 2016; Gao et al., 2016; Gerstner et al., 2014; Li et al., 2019; Lu et al., 2018; Zang et al., 2016; 2018; 2019a;b). In parallel with physical methods, learning system dynamics from abundant observations has drawn much attention, and the neural-based dynamics modeling method such as neural Ordinary Differential Equations (ODE) become the representative Chen et al. (2018).

To our knowledge, the basic idea of the representative method is to embed the original states of objects into a latent space before learning the dynamics using neural-based methods and finally followed by a decoder Zang & Wang (2020). Although the existing methods have been successfully applied in various systems, most of them must train a specific model given observations from different systems, resulting in limited generalizability. To meet this challenge, several recent studies investigate generic methods that can simultaneously handle multiple dynamics from various systems and environments Kirchmeyer et al. (2022); Huang et al. (2023). Unfortunately, due to the potential huge gap between various dynamics, developing generic dynamics modeling methods faces significant challenges and is still an open problem.

Inspired by the great success of pre-trained models, we raise a question: instead of developing generic dynamics modeling methods, whether we can conduct a generalized **P**re-trained **D**ynamic **E**nco**DER** (**PDEDER**), which, for various complex systems, can embed their original states into a latent space, where the dynamics can be more easily captured. To conduct this generalized PDEDER, we collect 153 sets of real-world and synthetic observations from 24 complex systems. Inspired by the success of time series forecasting using Pre-trained Language Models (PLM), we can employ any

PLM and further update it over these dynamic observations by tokenization techniques to achieve the generalized PDEDER. Given any future dynamic observation, we can fine-tune PDEDER with any specific dynamics modeling method. We evaluate PDEDER on 18 dynamic systems by long/short-term forecasting under both in-domain and cross-domain settings and the empirical results indicate the effectiveness of PDEDER.

In a nutshell, the major contributions of this paper can be outlined below:

- We propose a novel idea of updating PLM to build a generic encoder PDEDER for dynamics modeling.
- We collect extensive real-world and synthetic observations from various complex systems to train PDEDER.
- We conduct numbers of experiments to evaluate PDEDER on by long/short-term forecasting under both in-domain and cross-domain settings.

2 Related Work

Dynamics Modeling Methods Currently, mainstream dynamics modeling methods primarily fall into the data-driven manner. Zang & Wang (2020) combines neural ordinary differential equations Chen et al. (2018) with GNNs Wu et al. (2020) to approximate continuous-time dynamics of networks at an arbitrary time on the interaction graph. Shi et al. (2023) performs integral operations to the derivatives of the changing on time and spatial dimensions, demonstrating the ability of adapting to spatial and temporal dependencies. Huang et al. (2023) studies cross-environment learning of continuous multi-agent system dynamics. It models this using parameterized neural ordinary differential equations (ODEs)Chen et al. (2018), describing the dynamics of each system through shared ODE functions and environment-specific vectors for latent exogenous factors. Huang et al. (2020) learns dynamics from irregularly sampled partial observations. Wang & Yu (2023) argues that data-driven methods lack the ability of understanding hidden dynamics and responding to naturally occurring data distribution changes. It proposes incorporating prior physical knowledge into existing deep learning approaches to enhance model generalization in unknown environments. Kirchmeyer et al. (2022) associates different dynamics with multiple environments separately, adjusting the dynamic model based on context parameters specific to each environment, allowing for rapid adaptation and better generalization in low-sample environments. Gupta et al. (2022) decomposes complex systems into subsystems, modeling each subsystem as a neural ODE module and simulating various coupled topologies through the combination of these modules. Huang et al. (2024b) enhanced the modeling capability of physical systems through the time-reversal symmetry regularization term, improving the forecasting accuracy and robustness for complex systems.Luo et al. (2023) incorporates second-order graph convolution to capture non-neighborhood semantic information, as well as second-order graph ODEs to model higher-order temporal dependencies. Huang et al. (2024a)uses graph neural networks (GNN) as an ODE function to capture the dynamic effects of treatments over time and the combined effects of multiple treatments. Wu et al. (2024) provides a new approach for OOD fluid dynamics modeling and conducts extensive experiments on multiple benchmarks to validate the superiority of the method. Gravina et al. (2024) proposes to reinterpret existing graph neural networks as a discretized solution of an ODE, thereby extending them to handle graph streams with irregular sampling. Luo et al. (2024) proposed a novel graph ODE model that significantly enhances the modeling capability and generalization performance of multi-agent dynamical systems through the introduction of contextual prototypes.

Pre-trained Language Models for Time Series Forecasting Recently, PLMs have been successfully applied to various tasks. In handling sequence data tasks, Gruver et al. (2024) encodes time series as a string of numbers, forecasting the next token in the text to achieve sequence forecasting results, allowing time series input to adapt unilaterally to the input format of language models. PromptCast Xue & Salim (2023) converts the numerical inputs and outputs of time series into prompts, constructing forecasting tasks in a sentence-by-sentence manner. Nie et al. (2023) segments the time series into sub-sequence-level patches to serve as input for Transformers. AutoTimes Liu et al. (2024) transforms time series data into a format understandable by LLMs for auto-regressive forecasting. LLM4TS Chang et al. (2024) proposes a two-phase fine-tuning method, first aligning the model with the characteristics of the time series to better adapt the LLM, and then

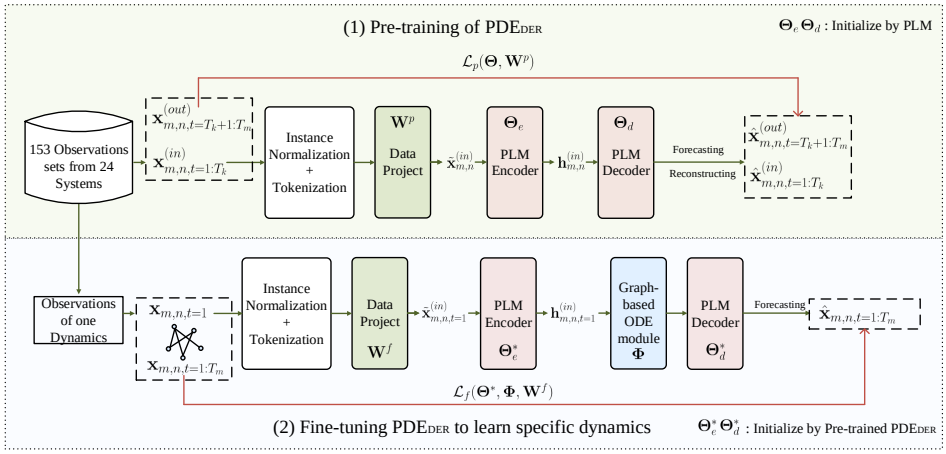

Figure 1: The flowchart of PDEDER.

further fine-tuning the model guided by downstream forecasting tasks in the second phase. Time-LLM Jin et al. (2024) requires no fine-tuning of any layers in the LLM, simply freezing the LLM and using two learnable modules to process inputs and outputs. Additionally, Zhou et al. (2023) provides a unified framework for various time series tasks. Zhang et al. (2024) proposed a framework that transitions from univariate pre-training to multivariate fine-tuning. Through self-supervised pre-training and cross-channel dependency fine-tuning, it demonstrates excellent performance across various time series tasks.

3 PRELIMINARIES

Commonly speaking, a dynamics contains a set of interacting objects whose states co-evolve over time on a weighted interaction graph. The dynamics could be formalized into a graph $\mathcal{G} = (\mathcal{V}, \mathcal{E})$, where the set of nodes $\mathcal{V} = \{\mathbf{x}_n\}_{n=1}^N$ consists of N interacting objects and $\mathcal{E} = \{\mathbf{e}_{i,j}\}_{i,j=1}^N$ denotes the interactions among them. The observations of each node $\mathbf{x}_n$ is a trajectory of states along time T. On time t, the state of object n can be represented as a vector $\mathbf{x}_{n,t} \in \mathbb{R}^V$ where V is the system-specific state dimension. The evolution of object states are governed by some hidden regularities for the most part. Given the states observations $\mathcal{G}$, we aim to extract the hidden governing dynamics and can help forecast the states at an arbitrary time t.

Ordinary Differential Equations (ODEs) for Dynamical System Conventionally, the evolution of each object states in a dynamics system can be described by Ordinary Differential Equations (ODEs): $\dot{\mathbf{x}}_{n,t} := \frac{d\mathbf{x}_{n,t}}{dt} = g(\mathbf{x}_{1,t}, \ldots, \mathbf{x}_{N,t}; \mathcal{G})$, where $g(\cdot; \mathcal{G})$ is a hand-crafted function to model the characteristic from the observations; $\mathcal{G}$ denotes the objects interactions. The differential equations describe the instantaneous changing rate of each object state under mutual influences. Given the initial states of each object $\{\mathbf{x}_{1,t=1}, \ldots, \mathbf{x}_{N,t=1}\}$, the states at an arbitrary time point τ can be calculated by integrating the differential equation over timeline:

$$\mathbf{x}_{n,\tau} = \mathbf{x}_{n,1} + \int_1^\tau g(\mathbf{x}_{1,t}, \ldots, \mathbf{x}_{N,t}; \mathcal{G}) dt. \tag{1}$$

The above integration is also called an ODE initial value problem Boyce et al. (2021) for this differential equation, which could be solved by numerical ODE solvers such as Euler's method, Dormand-Prince DOPRI5 Dormand (2018), Runge-Kutta Schober et al. (2019), *etc.* Then the dynamics model could be approximated with these numerical methods at an arbitrary time.

4 METHODOLOGY

4.1 OVERVIEW OF PDEDER

In this section, we introduce our proposed **P**re-trained **D**ynamic **E**nco**DER** (**PDEDER**). To learn an encoding model with outstanding generalizability, we first collect massive observations from both synthetic and real-world systems to ensure the diversity of training datasets. Then we pre-train PDEDER with the collected observations on two tasks. By ingesting the input observation into the model, we train PDEDER from two aspects, reconstructing the input observation, and forecasting unseen future states. With our pre-trained PDEDER, we can generate dynamics-enriched embeddings and approximate dynamics on these embeddings. Specifically, given the initial states of objects and their interactions, we encode the initial states by our pre-trained PDEDER into dynamics-enriched embeddings. Then we can learn dynamics on the interaction graph by approximating the observations using any dynamics modeling method. The flowchart is presented in Figure 1.

In this section, we first introduce the pre-training of our PDEDER. Secondly, we gave two examples of learning specific dynamics by fine-tuning PDEDER. We adopt two dynamics modeling methods as examples, including a black-box GNN-based neural method and a white-box method SINDy Brunton et al. (2021).

4.2 PRE-TRAINING OF THE PRE-TRAINED DYNAMIC ENCODER (PDEDER)

Benchmark Generation Firstly, we introduce the collection of dynamics observations. We collect 153 sets of observations including 122 synthetic sets from 14 systems with various hyper-parameters, and 31 sets of real-world observations from 10 systems. The domains consist of physics, fluid, biology, climate and traffic system. For each synthetic system $s \in [S]$, we set P_s different parameter settings, including numbers of objects and sequence lengths. For each parameter setting, we generate M_s sets of observations $\{\mathcal{G}_m = (\mathcal{V}_m, \mathcal{E}_m)\}_{m=1}^{M_s}$. $\mathcal{V}_m = \{\mathbf{x}_{m,n}\}_{n=1}^{N_m}$ denotes the observations of N_m objects and $\mathcal{E}_m = \{< \mathbf{x}_{m,i}, \mathbf{x}_{m,j} >\}_{i,j \in [N_m]}$ denotes the interactions among them. The observations $\mathbf{x}_{m,n} \in \mathbb{R}^{T_m \times V_s}$ of object n are denoted as a trajectory of states along time T_m, where V_s denotes the system-specific state dimension. For example, on system "Charged", we set 4 different numbers of objects $\{5, 10, 15, 20\}$ and 2 different sequence lengths $\{400, 600\}$. We generate 8 sets of observations using all combinations of the two sets of parameters. Each of the 8 sets corresponds with different system-specific hyper-parameters. Then we generate 5000 observation sequences under each parameter setting with random initial values. For all systems, we vary the number of objects and sequence length both from $[5, 1024]$. The statistics of observations are illustrated in Table 1 and the detailed descriptions of each system are presented in Appendix A. To pre-train PDEDER on multiple tasks, We split the observations $\mathbf{x}_{m,n}$ into two sub-observations $\mathbf{x}_{m,n}^{(in)} = \{\mathbf{x}_{m,n,t}\}_{t=1}^{t=T_k}$ and $\mathbf{x}_{m,n}^{(out)} = \{\mathbf{x}_{m,n,t}\}_{t=T_k+1}^{t=T_m}$. By ingesting the $\mathbf{x}_{m,n}^{(in)}$, we learn PDEDER by reconstructing $\mathbf{x}_{m,n}^{(in)}$ and forecasting $\mathbf{x}_{m,n}^{(out)}$.

Tokenization To adapt the input observations with various lengths and serve as input tokens for transformer-based PLMs, following Nie et al. (2023), we tokenize the observed states into sub-observations to adapt the input states with various lengths. For object n, we patch the input states $\mathbf{x}_{m,n}^{(in)} \in \mathbb{R}^{T_k \times V_s}$ into $\overline{\mathbf{x}}_{m,n}^{(in)} \in \mathbb{R}^{P_m \times L_p \times V_s}$, where L_p denotes the patch length; $P_m = \lfloor \frac{(T_k - L_p)}{R} \rfloor + 2$ denotes the number of patches and R denotes the stride. In this manner, the trajectory lengths are reduced by R times, which can simultaneously maintain the local semantics in long-term dynamics modeling and significantly reduce the space and time costs during model learning. Besides, to benefit domain adaptation and generalization, we add Gaussian noises and apply instance normalization before tokenization to handle the distribution shift among various domains following Kim et al. (2021).

Data Projection To handle dimension diversity of states across different systems, we adopt a flatten-linear data projection module to align the observations by mapping into same dimensions. For each patched tokens $\overline{\mathbf{x}}_{m,n}^{(in)} \in \mathbb{R}^{P_m \times L_p \times V_s}$, we first flatten it into $\overline{\mathbf{x}}_{m,n}^{(in)(fl)} \in \mathbb{R}^{P_m \times (L_p \cdot V_s)}$, and then project it by a linear layer into the dimension of L_p for all systems $\tilde{\mathbf{x}}_{m,n}^{(in)} = f(\overline{\mathbf{x}}_{m,n}^{(in)(fl)}; \mathbf{W}_{dp}^{s})$, where $\mathbf{W}_{dp}^{s} \in \mathbb{R}^{(L_p \cdot V_s) \times L_p}$ denotes the system-specific trainable parameters.

Table 1: Statistics of collected dynamics. N_m denotes the number of objects; T_m denotes the length of timestamp; V_s denotes the feature dimension; M_s denotes the number of samples generated; P_s denotes the number of different hyper-parameter settings.

System	Type	Domain	N_m	T_m	V_s	M_s	N_p
Charged	Synthetic	Physics	{5,10,15,20}	{400,600}	4	5000	8
Springs	Synthetic	Physics	{20,25,30,35,40}	{200,300}	4	3500	10
Mutualistic	Synthetic	Physics	{100,121,169,196,225}	{300,350,400}	1	1500	15
Heat	Synthetic	Physics	{225,256,289,324}	{200,250,300}	1	1500	12
1D Diff-Reaction	Synthetic	Fluid	{256,368,464,512}	{200,225,250,275}	1	700	16
1D CFD	Synthetic	Fluid	{300,350,400}	{600,625}	3	300	6
2D CFD	Synthetic	Fluid	{400,625,784,1024}	{100,150,200}	4	200	12
Burgers	Synthetic	Fluid	{400,425,450}	{512,768,960,1024}	1	250	12
Advection	Synthetic	Fluid	{500,550}	{700,725,750}	1	500	6
DarcyFlow	Synthetic	Fluid	{625,676}	{400,425,450}	1	700	6
Gene	Synthetic	Biology	{729,841,900,1024}	{125,150,175,200}	1	500	16
Shallow-Water	Synthetic	Fluid	768	500	1	3000	1
2D Diff-Reaction	Synthetic	Fluid	900	120	2	5000	1
Diff-Sorption	Synthetic	Fluid	1024	101	1	10000	1
LA	Real-world	Climate	274	384	10	1	-
SD	Real-world	Climate	282	384	10	1	-
NYCTaxi	Real-world	Traffic	75	17520	2	1	-
CHIBike	Real-world	Traffic	270	4416	2	1	-
TDrive	Real-world	Traffic	1024	3600	2	1	-
PEMS03	Real-world	Traffic	358	26208	1	1	-
PEMS04	Real-world	Traffic	307	16992	3	1	-
PEMS07	Real-world	Traffic	883	28224	1	1	-
PEMS08	Real-world	Traffic	170	17856	3	1	-
NOAA	Real-world	Climate	{17,24,27,29,40,40, 40,46,49,53,55,65, 77,89,93,108,160, 179,199,216,225,253}	7305	3	22	-

Learn with PLM With the projected $\tilde{\mathbf{x}}_{m,n}^{(in)}$, we reconstruct the input states and forecast future states by a pre-trained language model. First, we encode $\tilde{\mathbf{x}}_{m,n}^{(in)}$ by a convolutional layer $f(\cdot;\mathbf{W}_c)$ and the encoder of a PLM $f(\cdot;\mathbf{\Theta}_e)$. The convolutional layer is capable of maintaining the local semantic information and adapt the states dimension H into which of PLM Chang et al. (2023). Then, we decode the hidden features by the decoder of PLM $f(\cdot;\mathbf{\Theta}_d)$ attached by two flatten-linear layers $f(\cdot;\mathbf{W}_r^s)$ and $f(\cdot;\mathbf{W}_p^s)$, which serves for reconstructing and forecasting, respectively. Detailed calculations are as below:

$$\begin{gathered}\mathbf{h}_{m,n} = f(f(\tilde{\mathbf{x}}_{m,n}^{(in)};\mathbf{W}_c);\mathbf{\Theta}_e),\\ \hat{\mathbf{x}}_{m,n}^{(in)} = f(f(\mathbf{h}_{m,n};\mathbf{\Theta}_d);\mathbf{W}_r^s), \quad \hat{\mathbf{x}}_{m,n}^{(out)} = f(f(\mathbf{h}_{m,n};\mathbf{\Theta}_d);\mathbf{W}_p^s),\end{gathered} \tag{2}$$

Finally, the model is learnt by minimizing the reconstructing loss against the original input states $\mathbf{x}_{m,n}^{(in)}$ and the forecasting loss against the ground-truth future states $\mathbf{x}_{m,n}^{(out)}$:

$$\mathcal{L}_p(\mathbf{\Theta},\mathbf{W}^p) = \sum_{s=1}^{S}\sum_{p=1}^{P_s}\sum_{m=1}^{M_s}\sum_{n=1}^{N_m}\left(\sum_{t=1}^{T_k}\ell(\hat{\mathbf{x}}_{m,n,t}^{(in)},\mathbf{x}_{m,n,t}^{(in)}) + \sum_{t=T_k+1}^{T_m}\ell(\hat{\mathbf{x}}_{m,n,t}^{(out)},\mathbf{x}_{m,n,t}^{(out)})\right), \tag{3}$$

where $\ell(\cdot)$ denotes the L1 loss; $\mathbf{\Theta} = \{\mathbf{\Theta}_e, \mathbf{\Theta}_d\}$ denotes the parameters set of the encoder/decoder of the PLM; $\mathbf{W}^p = \{\mathbf{W}_{dp}^s, \mathbf{W}_c, \mathbf{W}_r^s, \mathbf{W}_p^s\}_{s=1}^S$.

4.3 Examples of Learning Specific Dynamics with PDEder

We now introduce the usage of PDEder when learning a specific dynamics. We introduce two examples of learning dynamics with a black-box GNN-based dynamics learner and a white-box dynamics learner SINDy Brunton et al. (2021).

Conventionally, given the observations of N_d objects $\{\mathbf{x}_{m,1}, \ldots, \mathbf{x}_{m,N_d}\}$ across time T_m, we can model the hidden dynamics by solving the ODE initial value problem with the initial observations $\{\mathbf{x}_{m,1,1}, \ldots, \mathbf{x}_{m,N_d,1}\}$ as mentioned in preliminaries. Following the pre-training processes in PDEDER, we tokenize and project the states into $\{\tilde{\mathbf{x}}_{m,1}, \ldots, \tilde{\mathbf{x}}_{m,N_d}\}$ and adopt the first token $\tilde{\mathbf{x}}_{m,n,1} \in \mathbb{R}^{L_p}$ as the initial value to learn dynamics. Then we encode the initial observations to $\mathbf{h}_{m,n,1} \in \mathbb{R}^H$ by the encoder of pre-trained PDEDER $\mathbf{h}_{m,n,1} = f(f(\tilde{\mathbf{x}}_{m,n,1}; \mathbf{W}_c); \mathbf{\Theta}_e^*)$, where $\mathbf{\Theta}_e^*$ denotes the pre-trained parameters of encoder in PDEDER.

Example: Fine-tune PDEDER with a Black-box Dynamics Learner. To model the dynamics where the objects affect each other along with evolution, following Zang & Wang (2020), we adapt a GNN-based module $g(\cdot)$ to model dynamics by incorporating the interactions among objects in the latent space. Let $\mathbf{A}_m \in \mathbb{R}^{N_m \times N_m}$ denotes the adjacent matrix of the interaction graph $\mathcal{G}_m$ and $\mathbf{h}_{m,\cdot,\tau} = [\mathbf{h}_{m,1,\tau}, \ldots, \mathbf{h}_{m,N_m,\tau}] \in \mathbb{R}^{N_m \times H}$ denotes the embeddings at an arbitrary time τ $(1 < \tau \leq T_m)$, we describe the dynamics by the following ODE:

$$\frac{d\mathbf{h}_{m,\cdot,\tau}}{dt} = g(\mathbf{h}_{m,\cdot,\tau}) = \psi(\mathbf{W}_g^\top \mathbf{\Lambda}_m \mathbf{h}_{m,\cdot,\tau}), \tag{4}$$

where $\mathbf{\Lambda}_m = \mathbf{D}_m^{-\frac{1}{2}}(\mathbf{D}_m - \mathbf{A}_m)\mathbf{D}_m^{-\frac{1}{2}} \in \mathbb{R}^{N_m \times N_m}$ denotes the Laplacian normalization of $\mathbf{A}_m$; $\mathbf{D}_m$ denotes the degree matrix of $\mathbf{A}_m$; $\mathbf{W}_g$ denotes the trainable parameters shared across timeline; $\psi(\cdot)$ denotes the ReLU activation function. With the above ODE, we can model the dynamics by integrating over continuous time:

$$\mathbf{h}_{m,\cdot,\tau} = \mathbf{h}_{m,\cdot,1} + \int_1^\tau \psi(\mathbf{W}_g^\top \mathbf{\Lambda}_m \mathbf{h}_{m,\cdot,t}) dt. \tag{5}$$

The hidden representations $\mathbf{h}_{m,\cdot,t}$ for all time points $t \in (1, T_m]$ could be calculated with the above integration. Then we reconstruct the states by the decoder of pre-trained PDEDER $\hat{\mathbf{x}}_{m,n} = f(f(\mathbf{h}_{m,n}; \mathbf{\Theta}_d^*); \mathbf{W}_r^s)$ and learn dynamics on system s by minimizing the forecasting loss against the ground-truth observations $\mathbf{x}_{m,n}$:

$$\mathcal{L}_f(\mathbf{\Theta}^*, \mathbf{\Phi}, \mathbf{W}^f) = \sum_{m=1}^{M_s} \sum_{n=1}^{N_m} \ell(\hat{\mathbf{x}}_{m,n}, \mathbf{x}_{m,n}), \tag{6}$$

where $\mathbf{\Theta}^* = \{\mathbf{\Theta}_e^*, \mathbf{\Theta}_d^*\}$ denotes the encoder (decoder) parameters of the pre-trained PDEDER; $\mathbf{\Phi} = \{\mathbf{W}_g\}$ denotes the parameters of the neural ODE module; $\mathbf{W}^f = \{\mathbf{W}_{dp}^s, \mathbf{W}_c, \mathbf{W}_r^s\}_{s=1}^S$.

4.4 MODEL TRAINING.

We first pre-train PDEDER on all collected dynamics observations (without graph) with Eq.3 for E_p epochs. To handle the massive observations and various numbers of samples on different systems, we randomly choose 10 dynamics systems for each training round and train PDEDER for 5 epochs with all the observations from these systems. When learning a specific dynamics, we fine-tune PDEDER with Eq.6 for E_f. The training details are presented in Algorithm 1 and 2.

5 EXPERIMENT

5.1 EXPERIMENTAL SETTINGS

Datasets In fine-tuning, we adopt 17 dynamics owning object interactions for validation, including 7 sets of synthetic observations: Mutualistic, Heat Diffusion, 2D Compressible Navier-Stokes, Darcy Flow, Gene, Shallow Water, 2D Diffusion Reaction; and 10 real-world observations: LA, SD, TDrive, CHIBike, NYCTaxi, PEMS03, PEMS04, PEMS07, PEMS08 and NOAA. Detailed descriptions are introduced in Appendix A.

Baselines We apply 5 baseline methods which models dynamics on interaction graph for comparison, including GNSSanchez-Gonzalez et al. (2020), NDCN Zang & Wang (2020), ST-GODE Fang et al. (2021), MT-GODE Jin et al. (2022) and TANGO Huang et al. (2024b). Following PDEDER, we adopt instance normalization on observations for all methods. Details of baseline methods are listed in Appendix B:

Algorithm 1 Pre-training PDEDER to learn dynamics-enriched embeddings.

Input: 153 Observations sets $\{\mathcal{V}_m\}_{m=1}^{M_s}$ from S systems
Output: Optimal parameters of PDEDER $\{\mathbf{\Theta}^*, \mathbf{W}^{p*}\}$

```
Initialize Θ by pre-trained LM;
for round r = 1 to MaxRound do
    Sample 10 systems for training;
    for epoch e = 1 to MaxEpoch_p do
        for iter it = 1 to MaxIter_p do
            Sample B observations from 10 systems as a batch by ratios ;
            Encode and decode observations by Eq.2;
            Calculate the pre-training objective of Eq.3;
            Update {Θ, W^p} by Eq.3;
        end for
    end for
end for
```

Algorithm 2 Fine-tuning PDEDER to learn specific dynamics.

Input: Observations $\{\mathcal{G}_m = (\mathcal{V}_m, \mathcal{E}_m)\}_{m=1}^{M_s}$ of a dynamics system s
Output: Optimal parameters of approximated dynamics $\mathbf{W}_g$

```
Initialize Θ by Θ*;
for epoch e = 1 to MaxEpoch_f do
    for iter it = 1 to MaxIter_f do
        Encode initial values by pre-trained PDEDER;
        Calculate integration for each time point by Eq.5;
        Calculate the fine-tuning objective of Eq.6;
        Update {Θ*, W_g, W^f} by Eq.6.
    end for
end for
```

Implementation Details We adopt the pre-trained `T5` to initialize the PLM module. We apply all available 153 sets of observations for pre-training PDEDER. To handle the massive observations and different numbers of samples on different systems, we randomly sample 10 sets of observations for each training round, and sample trajectories according to the proportions of their amounts. We train 5 epochs on each sets. The learning rates are set as $1e-3$ for the PLM module and $1e-2$ for rest parameters. The patch length and stride are set as 30 and 6, respectively. To align the observations with different lengths, we split each observation by a look-back window of length 150 and stride 50. T_k is set as 120.

In fine-tuning to learning a specific dynamics, the lengths of training observations is set as 60 for 2D Diffusion Reaction and 120 for the rest systems. The rest observations are left for testing. We fine-tune each observations for 20 epochs. The learning rates are tuned over $\{1e-4, 1e-5, 1e-6\}$ for the PLM module and $\{1e-2, 1e-3, 1e-4\}$ for rest parameters. The patch length and stride are set as 50 and 10, respectively. We adopt look-back window to handle overlong observations. The window length and stride are set as 840 and 50 for NYCTaxi, CHIBike, TDrive, PEMS03, PEMS04, PEMS07, PEMS08 and NOAA. Specifically, we adopt the last L_p states in training observations as initial states to forecast the test observations when fine-tuning PDEDER.

Short/Long-term Forecasting Settings The training sequence length are same for both short and long term forecasting. For NYCTaxi, CHIBike, TDrive, PEMS03, PEMS04, PEMS07, PEMS08 and NOAA, the short- and long-term forecasting lengths are set as $\{24, 48\}$ and $\{96, 192, 336, 720\}$. For the rest dynamics, due to the diversity of convergence characteristics on each system, we truncate the test sequences by ratios to form the short/long-term forecasting sequences. The ratios for short- and long-term are set as $\{10\%, 20\%\}$ and $\{50\%, 70\%, 80\%, 100\%\}$, respectively. For example, when the test sequence length is 200, we set $10\% \times 200 = 20$ and $20\% \times 200 = 40$ as the forecasting lengths.

Table 2: Average results of dynamics forecasting. The best scores are in **boldface**. % denotes the results are scaled by 1/100.

Short-term Forecasting

System	GNS			NDCN			ST-GODE			MT-GODE			PDEDER		
	MSE	MAE	MRAE	MSE	MAE	MRAE	MSE	MAE	MRAE	MSE	MAE	MRAE	MSE	MAE	MRAE
Mutualistic	0.283	0.418	1.717	0.424	0.542	3.560	1.058	0.901	2.729	0.961	0.781	1.299	0.362	0.452	5.761
Heat	0.113	0.280	0.510	0.490	0.551	2.903	0.676	0.666	3.813	0.910	0.795	1.968	0.003	0.045	0.286
2D CFD	0.302	0.383	31.315	0.490	0.482	8.418	0.566	0.434	1.518	0.546	0.432	12.360	0.223	0.303	1.185
DarcyFlow	0.233%	4.093%	1.077	0.524%	4.960%	21.085	0.195%	3.338%	10.209	0.660%	6.214%	23.893	0.067%	2.016%	1.398
Gene	0.045	0.116	0.757	0.616	0.644	1.919	0.841	0.755	2.924	0.805	0.661	1.006	0.035	0.136	1.513
ShallowWater	0.985	0.542	1.273	0.966	0.569	1.053	1.013	0.513	1.063	1.002	0.573	1.255	0.674	0.358	1.897
2D Diff-Reac	1.013	1.059	20.029	1.157	0.846	8.604	1.000	0.853	1.063	0.967	0.761	4.373	0.960	0.723	4.942
LA	0.493	0.489	3.552	0.993	0.789	2.563	0.944	0.713	3.320	1.077	0.780	2.499	0.581	0.516	2.325
SD	0.418	0.450	6.053	1.027	0.742	3.770	0.309	0.430	3.682	1.096	0.780	2.337	0.634	0.472	3.943
NYCTaxi	0.361	0.354	56.987	0.327	0.398	44.061	0.540	0.555	54.988	1.038	0.770	24.018	0.181	0.257	85.898
CHIBike	0.592	0.237	33.041	0.719	0.258	32.404	0.506	0.258	21.940	1.039	0.428	10.450	0.349	0.174	17.906
TDrive	0.302	0.290	16070.4	0.238	0.274	10110.9	0.461	0.459	28766.0	0.827	0.605	10122.5	0.119	0.169	15789.4
PEMS03	0.173	0.276	4.498	0.996	0.815	8.196	0.200	0.310	6.882	0.998	0.824	2.729	0.186	0.284	4.177
PEMS04	0.505	0.420	7.491	1.030	0.688	3.931	0.500	0.509	5.543	0.983	0.696	2.522	0.691	0.505	4.585
PEMS07	0.578	0.535	6.373	1.101	0.825	4.090	0.716	0.627	3.331	0.988	0.769	1.563	0.263	0.344	4.912
PEMS08	1.010	0.628	9.361	0.934	0.688	2.969	0.849	0.750	3.639	1.021	0.717	2.992	0.643	0.489	7.809
NOAA	0.503	0.521	11.201	0.585	0.570	19.107	0.585	0.572	2.905	0.957	0.712	5.669	0.362	0.432	19.468

Long-term Forecasting

System	GNS			NDCN			ST-GODE			MT-GODE			PDEDER		
	MSE	MAE	MRAE	MSE	MAE	MRAE	MSE	MAE	MRAE	MSE	MAE	MRAE	MSE	MAE	MRAE
Mutualistic	0.989	0.774	5.493	0.913	0.807	2.590	1.034	0.885	1.686	0.999	0.857	1.082	0.809	0.675	2.859
Heat	0.176	0.336	1.497	0.516	0.586	19.415	0.724	0.700	15.172	0.973	0.838	9.610	0.006	0.052	3.930
2D CFD	0.238	0.313	39.102	0.440	0.425	12.810	0.573	0.437	1.703	0.378	0.348	14.149	0.152	0.236	1.808
DarcyFlow	0.163%	3.254%	3.827	0.505%	4.909%	21.042	0.150%	2.901%	7.479	0.856%	7.305%	29.049	0.072%	2.064%	1.457
Gene	0.200	0.283	3.064	0.640	0.636	2.128	0.979	0.789	2.268	0.991	0.761	1.445	0.076	0.172	1.994
ShallowWater	1.002	0.545	1.316	0.993	0.578	1.018	1.012	0.513	1.046	1.006	0.579	1.134	1.145	0.527	1.960
2D Diff-Reac	1.007	1.060	10.992	1.133	0.837	5.076	1.001	0.852	1.129	1.005	0.792	2.535	1.057	0.794	4.037
LA	0.487	0.484	3.267	0.995	0.788	2.696	0.883	0.707	3.035	0.963	0.747	1.731	0.571	0.510	2.033
SD	0.428	0.454	7.476	1.027	0.747	3.285	0.332	0.444	3.175	0.968	0.741	2.008	0.642	0.482	3.764
NYCTaxi	0.361	0.354	61.015	0.340	0.406	55.474	0.580	0.579	63.998	1.018	0.763	11.699	0.208	0.271	53.717
CHIBike	0.598	0.237	69.580	0.722	0.259	60.684	0.536	0.263	93.543	1.015	0.422	15.124	0.350	0.178	62.679
TDrive	0.367	0.332	18430.2	0.303	0.320	14311.6	0.520	0.468	24255.0	0.898	0.646	7457.8	0.161	0.194	15649.1
PEMS03	0.303	0.385	5.766	1.122	0.872	7.408	0.205	0.317	7.102	1.016	0.840	2.755	0.302	0.378	7.305
PEMS04	0.742	0.548	14.116	1.026	0.687	4.195	0.394	0.456	5.569	1.003	0.708	2.483	0.836	0.586	6.029
PEMS07	0.575	0.533	7.386	1.090	0.820	4.594	0.715	0.627	3.282	1.000	0.781	1.761	0.435	0.464	6.400
PEMS08	1.006	0.625	12.804	0.935	0.688	3.822	0.872	0.757	4.179	1.008	0.715	2.805	0.763	0.565	8.161
NOAA	0.782	0.655	14.856	0.855	0.691	21.577	0.712	0.636	3.695	1.007	0.741	6.280	0.699	0.607	22.449

5.2 MODELING DYNAMICS

In-domain Forecasting We first examine PDEDER by short/long-term forecasting on in-domain settings against 4 baseline methods. We pre-train PDEDER on all 153 sets of observations and fine-tune on one set of observations for each system. We examine the performance by MSE and MAE. Due to the memory limitation, we compare with TANGO only on systems with less objects, including LA, NYCTaxi, PEMS08 and NOAA. The average results of short/long-term forecasting are presented in Table 2 and 6. The full results are presented in Appendix C. According to the forecasting results, we can find that our PDEDER outperforms baseline methods in most settings and improve the performance significantly. These observations directly indicate the effectiveness of our PDEDER which can approximate hidden dynamics elegantly in the latent space.

Cross-domain Forecasting We examine the generalizability of our PDEDER on cross-domain settings. We set two Leave-One-Out (LOO) cross-domain settings, leaving one system out and leaving one set of hyper-parameters out. For LOO on system s, we pre-train PDEDER by observations excluding all sets of observations on system s and fine-tune on one set of observations of system s for validation. For LOO on hyper-parameters, we pre-train PDEDER with observations excluding observations of a specific hyper-parameter $\mathcal{G}_m$ and fine-tune on $\mathcal{G}_m$ for validation. The two versions are denoted as "PDEDER-sys" and "PDEDER-para". We compare PDEDER with the two cross-domain

Table 3: Average results of short/long-term forecasting comparing in-domain and cross-domain settings. The best scores are in **boldface**. The dataset names are abbreviated for briefness. "N/A" denotes the system contains no system-specific hyper-parameters. "%" denotes the results are scaled by 1/100.

System	PDEDER						PDEDER-sys						PDEDER-para					
	short-term			long-term			short-term			long-term			short-term			long-term		
	MSE	MAE	MRAE	MSE	MAE	MRAE	MSE	MAE	MRAE	MSE	MAE	MRAE	MSE	MAE	MRAE	MSE	MAE	MRAE
Mutualistic	0.362	0.452	5.761	0.809	0.675	2.859	0.395	0.488	6.172	0.906	0.738	3.074	0.407	0.493	6.832	0.904	0.754	3.145
Heat	0.003	0.045	0.286	0.006	0.052	3.930	0.009	0.078	0.616	0.010	0.080	3.778	0.004	0.048	0.442	0.006	0.051	3.856
2D CFD	0.223	0.303	1.185	0.152	0.236	1.808	0.222	0.297	1.096	0.151	0.232	1.676	0.449	0.412	1.208	0.384	0.354	1.984
DarcyFlow	0.001	0.020	1.398	0.001	0.021	1.457	0.001	0.020	1.389	0.001	0.021	1.438	0.001	0.021	1.413	0.001	0.021	1.463
Gene	0.035	0.136	1.513	0.076	0.172	1.994	0.052	0.184	1.621	0.071	0.192	1.962	0.050	0.180	1.636	0.086	0.213	1.728
ShallowWater	0.674	0.358	1.897	1.145	0.527	1.960	0.773	0.368	1.304	1.032	0.464	1.448	N/A	N/A	N/A	N/A	N/A	N/A
2D Diff-Reac	0.960	0.723	4.942	1.057	0.794	4.037	0.972	0.727	5.268	1.034	0.786	3.748	N/A	N/A	N/A	N/A	N/A	N/A
LA	0.581	0.516	2.325	0.571	0.510	2.033	0.584	0.516	2.430	0.572	0.508	2.124	N/A	N/A	N/A	N/A	N/A	N/A
SD	0.634	0.472	3.943	0.642	0.482	3.764	0.641	0.479	3.985	0.648	0.487	3.741	N/A	N/A	N/A	N/A	N/A	N/A
NYCTaxi	0.181	0.257	85.898	0.208	0.271	53.717	0.192	0.266	87.668	0.217	0.278	54.779	N/A	N/A	N/A	N/A	N/A	N/A
CHIBike	0.349	0.174	17.906	0.350	0.178	62.679	0.308	0.167	19.382	0.333	0.175	62.413	N/A	N/A	N/A	N/A	N/A	N/A
Tdrive	0.119	0.169	15789.4	0.161	0.194	15649.1	0.118	0.171	16136.9	0.161	0.197	16000.9	N/A	N/A	N/A	N/A	N/A	N/A
PEMS03	0.186	0.284	4.177	0.302	0.378	7.305	0.188	0.288	4.629	0.308	0.384	7.871	N/A	N/A	N/A	N/A	N/A	N/A
PEMS04	0.691	0.505	4.585	0.836	0.586	6.029	0.681	0.497	4.555	0.832	0.583	6.104	N/A	N/A	N/A	N/A	N/A	N/A
PEMS07	0.263	0.344	4.912	0.435	0.464	6.400	0.233	0.324	4.664	0.431	0.464	6.715	N/A	N/A	N/A	N/A	N/A	N/A
PEMS08	0.643	0.489	7.809	0.763	0.565	8.161	0.639	0.490	8.181	0.762	0.566	8.305	N/A	N/A	N/A	N/A	N/A	N/A
NOAA	0.362	0.432	19.468	0.699	0.607	22.449	0.373	0.440	20.447	0.707	0.607	22.387	0.364	0.430	20.960	0.832	0.639	23.498

versions and present the averaged results of short/long-term forecasting in Table 3. Detailed results are presented in Appendix C. We can find that, the performance of in-domain setting outperforms the cross-domain settings in most cases. Meanwhile, the performance of excluding one system also beat the in-domain setting in some cases and the overall performance gaps are not too large. These phenomena indicate the strong generalizability of our PDEDER, even pre-training under cross-domain settings, our PDEDER can generate performance on a par with in-domain settings.

Impact Evaluation of Pre-training on downstream Dynamics Modeling We examine the impact of pre-training on downstream dynamics modeling by modifying the initialization of the encoder and decoder when fine-tuning. We set two comparable versions, 1) initializing PDEDER by pre-trained LM, denoted as "PDEDER w/o pre"; 2) initializing PDEDER by pre-trained

We conduct ablative study to examine the effectiveness of pre-training on PDEDER. We set two ablative versions: 1) fine-tuning PDEDER without pre-training, denoted as "PDEDER w/o pre"; 2) fine-tuning PDEDER with freezing the pre-trained encoder and decoder, denoted as "PDEDER freeze $\mathbf{\Theta}^*$". The averaged results are presented in Table 4 and full results are presented in Appendix C. We can find that the full version with pre-training PDEDER consistently outperforms the ablative versions, indicating the effectiveness of our pre-training mechanism on massive dynamics observations when learning hidden dynamics in latent space. Besides, we surprisingly find that the version freezing the pre-trained encoder and decoder outperforms the version without pre-training in most settings. This phenomena indicate that the pre-training processes can effectively capture the dynamics properties, leading to less efforts on fine-tuning processes when learning specific dynamics. According to these results, our PDEDER can be directly adopted as an effective embedder on learning specific dynamics in real-world applications when fine-tuning are unavailable.

Forecasting Visualization We present forecasting visualizations on Heat and Mutualistic on variants of PDEDER and the results are presented in Fig. 4 2 of Appendix. We may find that our PDEDER performs comparable dynamics behaviors against the ground-truth values.

Sensitivity Analysis WE conducted sensitivity analysis on the patch length and stride of fine-tuning period on Mutualistic, Heat, DarcyFlow, Gene and 2D Diffusion-Reaction. The results are presented in Fig. 3. We may find that the fine-tuning process are quite insensitive to these two parameters, leading to robustness in practical usages.

Prediction of Incidence Proportion We evaluate the performance of prediction on incidence proportions by MSE and MAE. Incidence Proportion (IP) Noordzij et al. (2010) measures the probability of a special event (*e.g.,* the infection of epidemic diseases) in a certain period. IP $= \frac{D_e}{D_o}$, where D_e denotes the number of occurrence of a certain event; D_o denotes the total number of monitored

Table 4: Average forecasting results of MSE and MAE under on Impact Evaluation of Pre-training on downstream Dynamics Modeling. The best scores are in **boldface**. The dataset names are abbreviated for briefness. "%" denotes the results are scaled by 1/100.

System	PDEDER						PDEDER w/o pre						PDEDER freeze Θ^*					
	short-term			long-term			short-term			long-term			short-term			long-term		
	MSE	MAE	MARE	MSE	MAE	MARE	MSE	MAE	MARE	MSE	MAE	MARE	MSE	MAE	MARE	MSE	MAE	MARE
Mutualistic	0.362	0.452	5.761	0.809	0.675	2.859	0.531	0.592	6.435	1.003	0.812	3.233	0.313	0.430	6.012	0.818	0.690	3.014
Heat	0.003	0.045	0.286	0.006	0.052	3.930	0.027	0.136	0.868	0.033	0.138	10.895	0.008	0.068	0.724	0.010	0.072	3.903
2D CFD	0.223	0.303	1.185	0.152	0.236	1.808	0.224	0.302	1.195	0.151	0.234	1.988	0.225	0.311	1.223	0.155	0.244	1.964
DarcyFlow	0.067%	2.016%	1.398	0.072%	2.064%	1.457	0.067%	2.023%	1.389	0.073%	2.086%	1.438	0.075%	2.108%	1.413	0.077%	2.141%	1.463
Gene	0.035	0.136	1.513	0.076	0.172	1.994	0.140	0.311	1.747	0.163	0.321	1.912	0.113	0.236	2.376	0.327	0.428	4.038
ShallowWater	0.674	0.358	1.897	1.145	0.527	1.960	1.000	0.416	1.091	1.057	0.437	1.122	0.754	0.371	1.244	1.034	0.478	1.456
2D Diff-Reac	0.960	0.723	4.942	1.057	0.794	4.037	0.981	0.737	5.265	1.006	0.777	3.523	0.958	0.730	4.634	1.009	0.778	3.372
LA	0.581	0.516	2.325	0.571	0.510	2.033	0.590	0.519	2.721	0.577	0.512	2.367	0.580	0.514	2.315	0.570	0.508	2.041
SD	0.634	0.472	3.943	0.642	0.482	3.764	0.666	0.500	4.093	0.675	0.509	3.733	0.642	0.480	4.007	0.652	0.490	3.805
NYCTaxi	0.181	0.257	85.898	0.208	0.271	53.717	0.188	0.265	87.134	0.219	0.284	55.841	0.212	0.297	64.056	0.224	0.286	47.551
CHIBike	0.349	0.174	17.906	0.350	0.178	62.679	0.510	0.212	23.712	0.414	0.191	76.088	0.417	0.194	18.753	0.388	0.185	61.128
Tdrive	0.119	0.169	15789.4	0.161	0.194	15649.1	0.165	0.214	19681.8	0.186	0.227	18089.6	0.152	0.194	15058.4	0.175	0.211	15216.5
PEMS03	0.186	0.284	4.177	0.302	0.378	7.305	0.202	0.311	4.729	0.333	0.408	8.353	0.186	0.295	4.488	0.302	0.382	7.392
PEMS04	0.691	0.505	4.585	0.836	0.586	6.029	0.703	0.520	5.121	0.875	0.609	6.799	0.678	0.500	4.574	0.835	0.587	6.115
PEMS07	0.263	0.344	4.912	0.435	0.464	6.400	0.302	0.386	5.670	0.494	0.509	7.513	0.238	0.326	5.077	0.426	0.461	6.547
PEMS08	0.643	0.489	7.809	0.763	0.565	8.161	0.670	0.525	9.137	0.824	0.607	9.616	0.641	0.489	7.956	0.759	0.564	8.247
NOAA	0.362	0.432	19.468	0.699	0.607	22.449	0.358	0.431	16.131	0.660	0.592	18.551	0.402	0.456	20.144	0.720	0.615	20.964

Table 5: Average results of predicted Incidence Proportion. The best scores are in **boldface**.

Method	PEMS03		PEMS04		PEMS07		PEMS08	
	short	long	short	long	short	long	short	long
NDCN	0.012	0.010	0.020	0.020	0.026	0.024	0.017	0.016
MTGODE	0.043	0.035	0.248	0.230	0.893	0.774	1.066	0.868
TANGO	OOM	OOM	OOM	OOM	OOM	OOM	5.210	6.646
PDEDER	**0.005**	**0.005**	**0.017**	**0.017**	**0.008**	**0.009**	**0.012**	**0.010**

subjects in the specified period. Following this, on traffic datasets, we calculate IP of traffice flows for each time point. We assign the object state at each time point to D_e and assign the states summation of all objects at one time point to D_o. We measure the predicted IP by MAE and the results are illustrated in Table 5. We can find that our PDEDER significantly outperforms baseline methods in all settings. This indicate that our PDEDER can serve as an effective forecaster for instance monitoring and warning in real-world applications.

6 CONCLUSION

In this paper, we propose a generalized pre-trained dynamics encoder PDEDER to learn generalizable embeddings for learning specific dynamics. During pre-training, we first collect 153 sets of dynamics observations from both synthetic and real-world systems. Then we pre-train a PLM-based PDEDER with all available observations by reconstructing and forecasting tasks to learn dynamics-enriched embeddings for each of the observations. Specifically, we introduce a data projection module for aligning states dimensions from different systems before the encoder. We also present the usage of fine-tuning PDEDER to learn specific dynamics. We encode the initial states by the pre-trained PDEDER and learn dynamics in latent space by a GNN-based ODE learner. We conducted empirical studies on short/long-term forecasting under in-domain and cross-domain settings. The results indicate the effectiveness and generality of our PDEDER. Specially, when freezing the pre-trained encoder (decoder) in fine-tuning, our PDEDER can also generate excellent performance, further indicating that PDEDER can serve as an effective embedder when fine-tuning are unavailabel.

REFERENCES

Uri Alon. An introduction to systems biology: Design principles of biological circuits. 2006.

Amir Bashan, Travis E Gibson, Jonathan Friedman, Vincent J Carey, Scott T Weiss, Elizabeth L Hohmann, and Yang-Yu Liu. Universality of human microbial dynamics. *Nature*, 534(7606): 259–262, 2016.

William E Boyce, Richard C DiPrima, and Douglas B Meade. *Elementary differential equations and boundary value problems*. John Wiley & Sons, 2021.

Steven L Brunton, Joshua L Proctor, and J Nathan Kutz. Discovering governing equations from data by sparse identification of nonlinear dynamical systems. *Proceedings of the National Academy of Sciences*, 113(15):3932–3937, 2021.

Ching Chang, Wen-Chih Peng, and Tien-Fu Chen. Llm4ts: Two-stage fine-tuning for time-series forecasting with pre-trained llms. *arXiv preprint arXiv:2308.08469*, 2023.

Ching Chang, Wei-Yao Wang, Wen-Chih Peng, and Tien-Fu Chen. Llm4ts: Aligning pre-trained llms as data-efficient time-series forecasters. *arXiv preprint arXiv:2308.08469*, 2024.

Chao Chen, Karl Petty, Alexander Skabardonis, Pravin Varaiya, and Zhanfeng Jia. Freeway performance measurement system: mining loop detector data. *Transportation research record*, 1748 (1):96–102, 2001.

Ricky TQ Chen, Yulia Rubanova, Jesse Bettencourt, and David K Duvenaud. Neural ordinary differential equations. *Advances In Neural Information Processing Systems*, 31, 2018.

Hwangyong Choi, Jeongwhan Choi, Jeehyun Hwang, Kookjin Lee, Dongeun Lee, and Noseong Park. Climate modeling with neural advection–diffusion equation. *Knowledge and Information Systems*, 65(6):2403–2427, 2023.

John R Dormand. *Numerical methods for differential equations: a computational approach*. CRC press, 2018.

Zheng Fang, Qingqing Long, Guojie Song, and Kunqing Xie. Spatial-temporal graph ode networks for traffic flow forecasting. In *Proceedings of the 27th ACM SIGKDD conference on knowledge discovery & data mining*, pp. 364–373, 2021.

Jianxi Gao, Baruch Barzel, and Albert-László Barabási. Universal resilience patterns in complex networks. *Nature*, 530(7590):307–312, 2016.

Wulfram Gerstner, Werner M Kistler, Richard Naud, and Liam Paninski. *Neuronal dynamics: From single neurons to networks and models of cognition*. Cambridge University Press, 2014.

Alessio Gravina, Daniele Zambon, Davide Bacciu, and Cesare Alippi. Temporal graph odes for irregularly-sampled time series. *arXiv preprint arXiv:2404.19508*, 2024.

Nate Gruver, Marc Finzi, Shikai Qiu, and Andrew G Wilson. Large language models are zero-shot time series forecasters. *Advances In Neural Information Processing Systems*, 36, 2024.

Jayesh Gupta, Sai Vemprala, and Ashish Kapoor. Learning modular simulations for homogeneous systems. *Advances In Neural Information Processing Systems*, 35:14852–14864, 2022.

Zijie Huang, Yizhou Sun, and Wei Wang. Learning continuous system dynamics from irregularly-sampled partial observations. *Advances In Neural Information Processing Systems*, 33:16177–16187, 2020.

Zijie Huang, Yizhou Sun, and Wei Wang. Generalizing graph ode for learning complex system dynamics across environments. In *Proceedings of the 29th ACM SIGKDD Conference on Knowledge Discovery and Data Mining*, pp. 798–809, 2023.

Zijie Huang, Jeehyun Hwang, Junkai Zhang, Jinwoo Baik, Weitong Zhang, Dominik Wodarz, Yizhou Sun, Quanquan Gu, and Wei Wang. Causal graph ode: Continuous treatment effect modeling in multi-agent dynamical systems. In *Proceedings of the ACM on Web Conference 2024*, pp. 4607–4617, 2024a.

Zijie Huang, Wanjia Zhao, Jingdong Gao, Ziniu Hu, Xiao Luo, Yadi Cao, Yuanzhou Chen, Yizhou Sun, and Wei Wang. Tango: Time-reversal latent graphode for multi-agent dynamical systems. *Advances In Neural Information Processing Systems*, in press, 2024b.

Jeehyun Hwang, Jeongwhan Choi, Hwangyong Choi, Kookjin Lee, Dongeun Lee, and Noseong Park. Climate modeling with neural diffusion equations. In *International Conference on Data Mining*, pp. 230–239, 2021.

Ming Jin, Yu Zheng, Yuan-Fang Li, Siheng Chen, Bin Yang, and Shirui Pan. Multivariate time series forecasting with dynamic graph neural odes. *IEEE Transactions on Knowledge and Data Engineering*, 35(9):9168–9180, 2022.

Ming Jin, Shiyu Wang, Lintao Ma, Zhixuan Chu, James Y Zhang, Xiaoming Shi, Pin-Yu Chen, Yuxuan Liang, Yuan-Fang Li, Shirui Pan, et al. Time-llm: Time series forecasting by reprogramming large language models. 2024.

Taesung Kim, Jinhee Kim, Yunwon Tae, Cheonbok Park, Jang-Ho Choi, and Jaegul Choo. Reversible instance normalization for accurate time-series forecasting against distribution shift. In *International Conference on Learning Representations*, 2021.

Thomas Kipf, Ethan Fetaya, Kuan-Chieh Wang, Max Welling, and Richard Zemel. Neural relational inference for interacting systems. In *International Conference on Machine Learning*, pp. 2688–2697, 2018.

Matthieu Kirchmeyer, Yuan Yin, Jérémie Donà, Nicolas Baskiotis, Alain Rakotomamonjy, and Patrick Gallinari. Generalizing to new physical systems via context-informed dynamics model. In *International Conference on Machine Learning*, pp. 11283–11301, 2022.

Gene A Klaasen and William C Troy. Stationary wave solutions of a system of reaction-diffusion equations derived from the fitzhugh–nagumo equations. *SIAM Journal on Applied Mathematics*, 44(1):96–110, 1984.

Haoyang Li, Peng Cui, Chengxi Zang, Tianyang Zhang, Wenwu Zhu, and Yishi Lin. Fates of microscopic social ecosystems: Keep alive or dead? In *International Conference on Machine Learning*, pp. 668–676. Proceedings of the 25th ACM SIGKDD International Conference on Knowledge Discovery & Data Mining, 2019.

Gaudet Limousin, J-P Gaudet, L Charlet, Stephanie Szenknect, V Barthes, and M Krimissa. Sorption isotherms: A review on physical bases, modeling and measurement. *Applied geochemistry*, 22 (2):249–275, 2007.

Lingbo Liu, Jiajie Zhen, Guanbin Li, Geng Zhan, Zhaocheng He, Bowen Du, and Liang Lin. Dynamic spatial-temporal representation learning for traffic flow prediction. 22:7169–7183, 2021.

Yong Liu, Guo Qin, Xiangdong Huang, Jianmin Wang, and Mingsheng Long. Autotimes: Autoregressive time series forecasters via large language models. *arXiv preprint arXiv:2402.02370*, 2024.

Yunfei Lu, Linyun Yu, Tianyang Zhang, Chengxi Zang, Peng Cui, Chaoming Song, and Wenwu Zhu. Collective human behavior in cascading system: discovery, modeling and applications. In *IEEE International Conference on Data Mining (ICDM)*, pp. 297–306, 2018.

Xiao Luo, Jingyang Yuan, Zijie Huang, Huiyu Jiang, Yifang Qin, Wei Ju, Ming Zhang, and Yizhou Sun. Hope: high-order graph ode for modeling interacting dynamics. In *Proceedings of the 40th International Conference on Machine Learning*, pp. 16. JMLR.org, 2023.

Xiao Luo, Yiyang Gu, Huiyu Jiang, Hang Zhou, Jinsheng Huang, Wei Ju, Zhiping Xiao, Ming Zhang, and Yizhou Sun. PGODE: Towards high-quality system dynamics modeling. In *Proceedings of the 41st International Conference on Machine Learning*, pp. 33305–33328. PMLR, 2024.

Yuqi Nie, Nam H Nguyen, Phanwadee Sinthong, and Jayant Kalagnanam. A time series is worth 64 words: Long-term forecasting with transformers. In *International Conference on Learning Representations*, 2023.

Marlies Noordzij, Friedo W. Dekker, Carmine Zoccali, and Kitty J. Jager. Measures of disease frequency: Prevalence and incidence. *Nephron Clinical Practice*, 115(1):c17–c20, 2010.

Alvaro Sanchez-Gonzalez, Jonathan Godwin, Tobias Pfaff, Rex Ying, Jure Leskovec, and Peter Battaglia. Learning to simulate complex physics with graph networks. In *International Conference on Machine Learning*, pp. 8459–8468, 2020.

Michael Schober, Simo Särkkä, and Philipp Hennig. A probabilistic model for the numerical solution of initial value problems. *Statistics and Computing*, 29(1):99–122, 2019.

Guangsi Shi, Daokun Zhang, Ming Jin, Shirui Pan, and Philip S Yu. Towards complex dynamic physics system simulation with graph neural odes. *arXiv preprint arXiv:2305.12334*, 2023.

Makoto Takamoto, Timothy Praditia, Raphael Leiteritz, Daniel MacKinlay, Francesco Alesiani, Dirk Pflüger, and Mathias Niepert. Pdebench: An extensive benchmark for scientific machine learning. *Advances in Neural Information Processing Systems*, 35:1596–1611, 2022.

A v Luikov. *Analytical heat diffusion theory*. Elsevier, 2012.

Jingyuan Wang, Jiawei Jiang, Wenjun Jiang, Chao Li, and Wayne Xin Zhao. Libcity: An open library for traffic prediction. In *Proceedings of the 29th international conference on advances in geographic information systems*, pp. 145–148, 2021.

Rui Wang and Rose Yu. Physics-guided deep learning for dynamical systems: A survey. abs/2107.01272, 2023.

Hao Wu, Huiyuan Wang, Kun Wang, Weiyan Wang, Changan Ye, Yangyu Tao, Chong Chen, Xian-Sheng Hua, and Xiao Luo. Prometheus: Out-of-distribution fluid dynamics modeling with disentangled graph ODE. In *International Conference on Machine Learning*, pp. 53870–53891, 2024.

Zonghan Wu, Shirui Pan, Fengwen Chen, Guodong Long, Chengqi Zhang, and S Yu Philip. A comprehensive survey on graph neural networks. *IEEE Transactions On Neural Networks And Learning Systems*, 32(1):4–24, 2020.

Hao Xue and Flora D Salim. Promptcast: A new prompt-based learning paradigm for time series forecasting. *IEEE Transactions on Knowledge and Data Engineering*, 2023.

Chengxi Zang and Fei Wang. Neural dynamics on complex networks. In *Proceedings of the 26th ACM SIGKDD International Conference on Knowledge Discovery & Data Mining*, pp. 892–902, 2020.

Chengxi Zang, Peng Cui, and Christos Faloutsos. Beyond sigmoids: The nettide model for social network growth, and its applications. In *Proceedings of the 22nd ACM SIGKDD International Conference on Knowledge Discovery and Data Mining*, pp. 2015–2024, 2016.

Chengxi Zang, Peng Cui, Christos Faloutsos, and Wenwu Zhu. On power law growth of social networks. *IEEE Transactions on Knowledge and Data Engineering*, 30(9):1727–1740, 2018.

Chengxi Zang, Peng Cui, Chaoming Song, Wenwu Zhu, and Fei Wang. Uncovering pattern formation of information flow. In *Proceedings of the 25th ACM SIGKDD International Conference on Knowledge Discovery & Data Mining*, pp. 1691–1699, 2019a.

Chengxi Zang, Peng Cui, Wenwu Zhu, and Fei Wang. Dynamical origins of distribution functions. In *Proceedings of the 25th ACM SIGKDD International Conference on Knowledge Discovery & Data Mining*, pp. 469–478, 2019b.

Yunhao Zhang, Minghao Liu, Shengyang Zhou, and Junchi Yan. UP2ME: Univariate pre-training to multivariate fine-tuning as a general-purpose framework for multivariate time series analysis. In *International Conference on Machine Learning (ICML)*, 2024.

Tian Zhou, Peisong Niu, Liang Sun, Rong Jin, et al. One fits all: Power general time series analysis by pretrained lm. *Advances in neural information processing systems*, 36:43322–43355, 2023.

GENERALIZING DYNAMICS MODELING EASIER FROM REPRESENTATION PERSPECTIVE: APPENDIX

A DYNAMICS

We introduce the dynamics we adopted for generating observations and the descriptions on synthetic systems.

Charged Similar to the Springs dataset, the Charged dataset Kipf et al. (2018) simulates the motion of charges in a two-dimensional bounded space. Five charges interact with each other through Coulomb forces, with the magnitude of the force being influenced by the distance between the charges. The expression for the Coulomb force is as follows, where C is a constant.

$$\mathbf{F}_{ij} = C \cdot \text{sign}(\mathbf{q}_i \cdot \mathbf{q}_j) \frac{\mathbf{r}_i - \mathbf{r}_j}{\|\mathbf{r}_i - \mathbf{r}_j\|^3}. \tag{7}$$

Springs Five particles move in a two-dimensional bounded space without external forces Kipf et al. (2018). The probability of randomly connecting each pair of particles with a spring is 0.5. Particles connected by springs will be influenced by Hooke's law $\mathbf{F}_{m,n} = -k(\mathbf{r}_m - \mathbf{r}_n)$, where $\mathbf{F}_{m,n}$ is the force exerted by particle v_m on particle v_n, and $\mathbf{r}_m$ is the position vector of particle v_m. The initial position of each particle is sampled from $N(0, 0.5)$, and the initial velocity is a random vector with a norm of 0.5.

Mutualistic Interaction Dynamics In the field of ecology, species interact with each other, and the expression Gao et al. (2016) is given as below :

$$\frac{d\mathbf{x_i(t)}}{dt} = b_i + \mathbf{x_i}\left(1 - \frac{\mathbf{x}_i}{k_i}\right)\left(\frac{\mathbf{x}_i}{c_i} - 1\right) + \sum_{j=1}^{n} \mathbf{A}_{i,j} \frac{\mathbf{x}_i \mathbf{x}_j}{d_i + e_i \mathbf{x}_i + h_j \mathbf{x}_j}. \tag{8}$$

We denote $\mathbf{x_i}$ represents the abundance of species i, b_i denotes the immigration term, k_i represents the logarithmic growth of population capacity, c_i indicates the Allee effect with a cold-start threshold, and $\mathbf{A}$ is the interaction network with interaction terms.

Heat Diffusion The heat diffusion dynamics is governed by Newton's law of cooling v Luikov (2012). The expression is given as below:

$$\frac{d\mathbf{x}_n^t}{dt} = -k_{nn'} \sum_{n' \in \mathcal{N}(n)} \mathbf{A}_{nn'}(\mathbf{x}_n - \mathbf{x}_{n'}). \tag{9}$$

Let $\mathbf{A}$ denotes the heat capacity matrix, for object n, the corresponding heat change is proportional to the temperature differences between object n and its corresponding neighbor objects $n' \in \mathcal{N}(n)$.

1D Diffusion-Reaction In the one-dimensional diffusion-reaction equation Takamoto et al. (2022),with the specific expression as follows:

$$\begin{aligned} \partial_t u(t,x) - \nu \partial_{xx} u(t,x) - \rho u(1-u) = 0, \quad x \in (0,1),\ t \in (0,1], \\ u(0,x) = u_0(x), \quad x \in (0,1). \end{aligned} \tag{10}$$

In the equation, the variable u is used to represent the ability to capture fast dynamics, where periodicity and initial conditions known to the advection equation are used

Compressible Navier-Stokes The flow of compressible fluids is generally represented by compressible fluid dynamics equations Klaasen & Troy (1984), which are expressed as follows:

$$\begin{aligned} &\partial_t \rho + \nabla \cdot (\rho \mathbf{v}) = 0, \\ &\rho(\partial_t \mathbf{v} + \mathbf{v} \cdot \nabla \mathbf{v}) = -\nabla p + \eta \Delta \mathbf{v} + \left(\zeta + \frac{\eta}{3}\right) \nabla(\nabla \cdot \mathbf{v}), \\ &\partial_t \left[\epsilon + \frac{\rho v^2}{2}\right] + \nabla \cdot \left[\left(\epsilon + p + \frac{\rho v^2}{2}\right)\mathbf{v} - \mathbf{v} \cdot \boldsymbol{\sigma}\right] = 0, \end{aligned} \tag{11}$$

where ρ represents mass density, v denotes velocity, p is the pressure, ϵ signifies internal energy, σ represents the viscous tensor, η is the shear viscosity, ζ is the bulk viscosity, and $M = \frac{|\mathbf{v}|}{c_s}$ denotes the Mach number. Following Takamoto et al. (2022), we abbreviate this dynamics as "CFD" for briefness.

Burgers The Burgers' equation is used to describe nonlinear behavior and diffusion processes in fluid dynamics Takamoto et al. (2022). Define the specific equation as follows:

$$\begin{gathered}\partial_t u(t,x) + \partial_x \left(\frac{u^2(t,x)}{2}\right) = \frac{\nu}{\pi}\partial_{xx} u(t,x), \quad x \in (0,1),\ t \in (0,2], \\ u(0,x) = u_0(x), \quad x \in (0,1).\end{gathered} \tag{12}$$

Here, v is the diffusion coefficient, which is a constant, and the same initial conditions as those used for advection are applied.

Advection The advection equation is used to simulate nonlinear advection behavior Takamoto et al. (2022). The specific equation is as follows:

$$\begin{gathered}\partial_t u(t,x) + \beta \partial_x u(t,x) = 0, \quad x \in (0,1),\ t \in (0,2], \\ u(0,x) = u_0(x), \quad x \in (0,1).\end{gathered} \tag{13}$$

Set β as the advection velocity, using the sine wave's hyperposition as the initial condition $u_0(x)$.

Gene Regulatory The dynamics of gene regulation are governed by the Michaelis-Menten equation, as specifically shown below Gao et al. (2016).

$$\frac{d\mathbf{x_n(t)}}{dt} = -b_n \mathbf{x}_n^f + \sum_{n'=1}^{m} \mathbf{A}_{n,n'} \frac{\mathbf{x_n}'^h}{\mathbf{x}_{n'}^h + 1}. \tag{14}$$

In the first term, f takes the values of 1 or 2, representing degradation and dimerization, respectively. The second term reflects genetic activation regulated by the Hill coefficient h Alon (2006).

Shallow-Water The architectures chosen to simulate free surface flow problems are mostly derived from the Navier-Stokes equations. The specific equation is shown below:

$$\begin{gathered}\partial_t h + \partial_x (hu) + \partial_y (hv) = 0, \\ \partial_t (hu) + \partial_x \left(u^2 h + \frac{1}{2} g_r h^2\right) + \partial_y (uvh) = -g_r h \partial_x b, \\ \partial_t (hv) + \partial_y \left(v^2 h + \frac{1}{2} g_r h^2\right) + \partial_x (uvh) = -g_r h \partial_y b,\end{gathered} \tag{15}$$

where u and v represent the horizontal and vertical velocities, respectively, h denotes the water depth, b indicates spatial variations, and g_r is the gravitational acceleration. The terms h_u and h_v represent the components of momentum in the horizontal and vertical directions Takamoto et al. (2022).

2D Diffusion-Reaction The diffusion-reaction equation in two-dimensional space is defined as follows Takamoto et al. (2022):

$$\begin{gathered}\partial_t u = D_u \partial_{xx} u + D_u \partial_{yy} u + R_u, \\ \partial_t v = D_v \partial_{xx} v + D_v \partial_{yy} v + R_v,\end{gathered} \tag{16}$$

where the activator is represented by u and the inhibitor by v. D_u and D_v are the diffusion coefficients for both, while R_u and R_v are the reaction functions Klaasen & Troy (1984), which are defined as follows:

$$\begin{gathered}R_u(u,v) = u - u^3 - k - v, \\ R_v(u,v) = u - v.\end{gathered} \tag{17}$$

We set the constants $k = 5 \times 10^{-3}, D_u = 1 \times 10^{-3}, D_v = 5 \times 10^{-3}$.

Diffusion-Sorption The diffusion process delayed by adsorption is typically described by the diffusion-adsorption equation. The equation is defined as follows:

$$\begin{aligned} \partial_t u(t,x) &= \frac{D}{R(u)} \partial_{xx} u(t,x), \quad x \in (0,1),\ t \in (0,500], \\ R(u) &= 1 + \frac{1-\varphi}{\varphi} \rho_s k n_f u^{n_f - 1}, \end{aligned} \tag{18}$$

where D represents the diffusion coefficient, while R denotes the delay factor of adsorption that hinders the diffusion process, with the value of R being dependent on u. The parameter ϖ represents the porosity of the porous medium, ρ_s represents the packing density, k is the Freundlich parameter, and n is the Freundlich index Limousin et al. (2007).

LA and SD The dataset collected hourly climate observation data for six consecutive days in Los Angeles and San Diego (from June 28, 2012, at 21:00 to July 14, 2012, at 22:00), with each node containing 10 observation values Choi et al. (2023). The interaction graph structures are provided by the original datasets.

NYCTaxi ,TDrive and CHIBike The NYCTaxi dataset Liu et al. (2021) contains bicycle trajectory data for 182 days in New York City, along with 4,392 traffic flow images.The TDrive dataset Liu et al. (2021) contains a large number of GPS trajectories from taxis in Beijing, along with 22,459 traffic flow images. The CHIBike dataset is sourced fromWang et al. (2021). The interaction graph structures are calculated by the geometry coordinate or grid distances between each station.

PEMS The PeMS dataset is real-world traffic data collected by the California Department of Transportation Chen et al. (2001) and contains three traffic measurements, separated at five-minute intervals. The interaction graph structures are provided by the original datasets.

NOAA Following Hwang et al. (2021), we randomly select 22 areas on the map of America and collect hourly temperatures from Online Climate Data Directory of the National Oveanic and Atmospheric Administration (NOAA)[1]. The interaction graph structures are calculated by the geometry coordinate distances between each station.

B BASELINE METHODS

Details of baseline methods are listed below:

- GNS[2] Sanchez-Gonzalez et al. (2020) is a discrete GNN-based dynamics modeling method. We modify the graph learning module into static graph structures.
- NDCN[3] Zang & Wang (2020) combines the ODEs with GNNs and approximate the integration differential equation systems by the GNN module. In testing, we set the state of the last time point of training observations as the initial states to forecast the test observations. We set the state of the last time point of training observations as the initial states for testing.
- STGODE[4] Fang et al. (2021) incorporates the geometry spatial information into continuous dynamics learning. STGODE constructs two types of graphs, including spatial and semantic correlations to capture the spatial temporal semantics by a continuous GNN with residual connections.
- MT-GODE[5] Jin et al. (2022) solves the multivariate time series forecasting by mapping the interacting observations into dynamic-graph and solve by learning continuous spatial-temporal dynamics in latent space. We adopt the single-step forecasting setting.

[1] https://www.ncdc.noaa.gov/cdo-web/
[2] https://github.com/zhouxian/GNS-PyTorch
[3] https://github.com/calvin-zcx/ndcn
[4] https://github.com/square-coder/STGODE
[5] https://github.com/TrustAGI-Lab/MTGODE

Table 6: Average results of short/long-term forecasting comparing with TANGO. Due to the memory limitation, we compare with TANGO only on systems with less objects. The best scores are in **boldface**.

System	TANGO				PDEDER			
	short-term		long-term		short-term		long-term	
	MSE	MAE	MSE	MAE	MSE	MAE	MSE	MAE
LA	0.761	0.685	0.699	0.649	0.574	0.509	**0.561**	**0.502**
NYCTaxi	1.051	0.793	2.459	1.207	**0.184**	**0.261**	**0.208**	**0.273**
CHIBike	0.453	0.391	1.231	0.621	**0.339**	**0.174**	**0.345**	**0.178**
PEMS08	1.034	0.810	2.878	1.233	0.639	0.489	**0.765**	**0.568**
NOAA	1.064	0.809	1.965	1.031	**0.351**	**0.422**	**0.687**	**0.597**

Table 7: Average results of short/long-term forecasting comparing fine-tuning PDEDER by GNN-based module and SINGy. The best scores are in **boldface**.

System	PDEDER				PDEDER +SINDy			
	short-term		long-term		short-term		long-term	
	MSE	MAE	MSE	MAE	MSE	MAE	MSE	MAE
Mutualistic	0.362	0.452	0.809	0.675	1.014	1.014	0.334	0.334
Heat	0.003	0.045	0.006	0.052	0.886	0.884	1.577	1.586
2D CFD	0.223	0.303	0.152	0.236	1.001	0.984	1.139	1.164
DarcyFlow	0.001	0.020	0.001	0.021	0.858	0.851	1.103	1.104
Gene	0.035	0.136	0.076	0.172	0.613	0.537	0.783	0.783
Shallow Water	0.674	0.358	1.145	0.527	0.538	0.463	1.040	1.047
2D DiffReac	0.960	0.723	1.057	0.794	0.126	0.126	0.807	0.808

- TANGO[6] Huang et al. (2024b) introduce time-reversal symmetry into GNN-based ODE learner and models the observations and reversed observations simultaneously. In the period of model training, we set the observations of the first 60 lengths as observed states to forecast the latter 60 observations. In model testing, we set the last 40 lengths of training observations as observed initial states to forecast the test observations. Specially, due to the memory limitation, we only compare with TANGO on systems with less objects.

C FULL RESULTS OF SHORT/LONG-TERM FORECASTING

The full results for forecasting are presented in Tables 8,9, 10, 11, including the variants results and cross-domain results. The variant without pre-training of PDEDER is denoted as "PDEDER-nopre". The variant freezes the encoder/decoder of PDEDER is denoted as "PDEDER-frz". The variant pre-trains PDEDER excluding one system on cross-domain setting is denoted as "PDEDER-sys"

[6] https://github.com/wanjiaZhao1203/TREAT

Table 8: Full results of short/long-term forecasting comparing with baselines (1/2). The best scores are in **boldface**. The dataset names are abbreviated for briefness. "%" denotes the results are scaled by 1/100.

System		NDCN			GNS			ST-GODE			MT-GODE			PDEDER		
		MSE	MAE	MRAE	MSE	MAE	MRAE	MSE	MAE	MRAE	MSE	MAE	MRAE	MSE	MAE	MRAE
Mutualistic	10%	0.166	0.338	1.031	0.328	0.475	2.840	1.064	0.909	2.875	0.947	0.792	1.297	0.276	0.386	5.702
	20%	0.399	0.498	2.402	0.520	0.609	4.281	1.051	0.894	2.584	0.976	0.769	1.302	0.448	0.518	5.820
	50%	0.886	0.733	5.202	0.855	0.770	3.221	1.040	0.878	1.985	0.998	0.833	1.118	0.750	0.656	3.675
	70%	0.984	0.773	5.361	0.912	0.806	2.599	1.035	0.884	1.690	0.997	0.856	1.082	0.813	0.679	2.879
	80%	1.017	0.785	5.391	0.930	0.817	2.405	1.033	0.887	1.598	0.998	0.864	1.071	0.829	0.683	2.625
	100%	1.069	0.806	6.017	0.956	0.833	2.134	1.029	0.890	1.470	1.002	0.877	1.058	0.844	0.683	2.259
Heat	10%	0.112	0.284	0.542	0.483	0.545	2.613	0.668	0.661	3.114	0.877	0.774	1.847	0.003	0.045	0.307
	20%	0.114	0.276	0.478	0.498	0.558	3.192	0.683	0.672	4.511	0.943	0.817	2.088	0.003	0.045	0.264
	50%	0.135	0.290	0.920	0.512	0.579	9.268	0.710	0.690	8.326	0.967	0.834	8.384	0.004	0.048	0.885
	70%	0.161	0.321	1.418	0.518	0.587	19.715	0.727	0.702	15.480	0.978	0.841	9.091	0.005	0.051	3.719
	80%	0.180	0.343	1.644	0.519	0.589	22.421	0.730	0.704	17.535	0.980	0.842	9.893	0.006	0.052	4.536
	100%	0.227	0.392	2.008	0.516	0.589	26.257	0.729	0.705	19.346	0.968	0.836	11.070	0.009	0.059	6.581
2D CFD	10%	0.308	0.390	28.476	0.486	0.483	8.452	0.575	0.439	1.544	0.611	0.457	12.435	0.230	0.309	1.158
	20%	0.295	0.376	34.153	0.494	0.480	8.384	0.557	0.429	1.492	0.480	0.406	12.285	0.216	0.296	1.212
	50%	0.260	0.339	39.077	0.465	0.449	11.434	0.553	0.425	1.671	0.403	0.368	13.364	0.177	0.261	1.539
	70%	0.241	0.317	37.658	0.444	0.429	12.306	0.564	0.432	1.697	0.377	0.348	12.581	0.155	0.240	1.715
	80%	0.232	0.307	38.380	0.434	0.419	12.745	0.579	0.441	1.727	0.370	0.341	14.436	0.146	0.230	1.861
	100%	0.218	0.288	41.295	0.415	0.401	14.753	0.598	0.452	1.717	0.363	0.335	16.217	0.130	0.212	2.118
DarcyFlow	10%	0.241%	4.178%	1.069	0.532%	4.981%	21.489	0.192%	3.404%	10.887	0.522%	5.580%	21.086	0.065%	1.998%	1.404
	20%	0.226%	4.008%	1.084	0.516%	4.939%	20.680	0.197%	3.272%	9.532	0.797%	6.848%	26.700	0.069%	2.034%	1.392
	50%	0.186%	3.545%	1.169	0.507%	4.914%	21.351	0.162%	2.992%	7.970	0.845%	7.193%	28.617	0.072%	2.063%	1.486
	70%	0.166%	3.288%	1.308	0.505%	4.909%	20.978	0.148%	2.888%	7.462	0.857%	7.320%	28.951	0.072%	2.065%	1.468
	80%	0.157%	3.180%	1.452	0.505%	4.908%	21.000	0.148%	2.887%	7.384	0.897%	7.497%	29.882	0.072%	2.065%	1.449
	100%	0.144%	3.004%	11.379	0.504%	4.906%	20.839	0.142%	2.836%	7.100	0.825%	7.211%	28.746	0.072%	2.065%	1.426
Gene	10%	0.038	0.100	0.645	0.596	0.633	1.854	0.841	0.764	2.838	0.752	0.618	0.974	0.033	0.135	1.528
	20%	0.053	0.132	0.870	0.636	0.654	1.984	0.841	0.746	3.010	0.858	0.705	1.038	0.036	0.138	1.499
	50%	0.121	0.220	2.048	0.648	0.650	2.199	0.901	0.762	2.332	0.977	0.760	1.567	0.052	0.152	1.796
	70%	0.182	0.273	2.897	0.643	0.639	2.136	0.961	0.782	2.207	0.990	0.763	1.451	0.069	0.167	1.928
	80%	0.214	0.297	3.346	0.639	0.633	2.067	0.994	0.793	2.252	0.998	0.763	1.406	0.079	0.176	1.985
	100%	0.283	0.342	3.966	0.631	0.622	2.111	1.062	0.818	2.282	0.997	0.758	1.357	0.103	0.194	2.268
ShallowWater	10%	0.982	0.541	0.804	0.955	0.565	1.057	1.012	0.515	0.893	0.998	0.571	1.306	0.582	0.327	1.611
	20%	0.988	0.542	1.741	0.978	0.572	1.049	1.014	0.510	1.232	1.005	0.576	1.204	0.766	0.389	2.183
	50%	0.997	0.544	1.303	0.991	0.577	1.023	1.012	0.514	1.021	1.006	0.580	1.132	1.085	0.500	1.930
	70%	1.001	0.545	1.334	0.993	0.578	1.019	1.012	0.514	1.033	1.006	0.578	1.125	1.152	0.529	1.938
	80%	1.003	0.545	1.273	0.994	0.578	1.017	1.013	0.513	1.008	1.006	0.579	1.120	1.165	0.536	1.866
	100%	1.006	0.545	1.355	0.995	0.579	1.015	1.012	0.513	1.122	1.006	0.579	1.158	1.179	0.543	2.106
2D DiffReac	10%	1.013	1.061	24.661	1.168	0.850	10.476	1.000	0.854	1.046	0.949	0.747	5.338	0.945	0.715	4.918
	20%	1.012	1.057	15.398	1.146	0.841	6.732	1.001	0.853	1.080	0.985	0.775	3.408	0.975	0.731	4.965
	50%	1.006	1.060	11.152	1.135	0.837	5.386	1.001	0.852	1.108	1.000	0.789	2.744	1.061	0.789	4.292
	70%	1.007	1.060	11.343	1.133	0.837	5.156	1.001	0.852	1.146	1.006	0.792	2.576	1.053	0.792	4.123
	80%	1.007	1.060	11.107	1.132	0.836	4.989	1.001	0.852	1.135	1.007	0.793	2.433	1.055	0.795	3.984
	100%	1.006	1.061	10.366	1.131	0.836	4.775	1.001	0.852	1.128	1.008	0.794	2.387	1.061	0.800	3.751
LA	10%	0.486	0.485	3.696	0.992	0.789	2.552	0.936	0.701	3.387	1.126	0.794	2.873	0.581	0.516	2.405
	20%	0.500	0.494	3.408	0.994	0.789	2.574	0.953	0.725	3.252	1.027	0.766	2.126	0.582	0.516	2.245
	50%	0.491	0.488	3.405	0.995	0.789	2.625	0.910	0.716	3.133	0.971	0.750	1.780	0.575	0.512	2.087
	70%	0.486	0.484	3.338	0.995	0.788	2.666	0.883	0.706	3.092	0.963	0.747	1.719	0.572	0.510	2.039
	80%	0.487	0.484	3.234	0.995	0.788	2.793	0.879	0.707	3.007	0.961	0.746	1.718	0.570	0.509	2.019
	100%	0.483	0.481	3.090	0.995	0.787	2.700	0.861	0.701	2.907	0.957	0.745	1.707	0.568	0.508	1.988
SD	10%	0.408	0.443	5.532	1.027	0.741	4.052	0.304	0.427	3.838	1.149	0.797	2.285	0.634	0.472	2.958
	20%	0.429	0.456	6.573	1.027	0.743	3.489	0.314	0.434	3.526	1.043	0.763	2.388	0.634	0.473	4.927
	50%	0.425	0.454	7.190	1.027	0.746	3.391	0.319	0.434	3.228	0.980	0.746	2.113	0.639	0.478	4.018
	70%	0.424	0.453	7.637	1.027	0.747	3.241	0.330	0.444	3.120	0.968	0.742	1.976	0.642	0.481	3.749
	80%	0.430	0.456	7.557	1.027	0.748	3.225	0.335	0.446	3.084	0.966	0.741	2.014	0.643	0.483	3.677
	100%	0.431	0.455	7.520	1.026	0.747	3.282	0.345	0.453	3.267	0.958	0.736	1.929	0.644	0.484	3.613
NYCTaxi	24	0.360	0.354	72.023	0.323	0.396	51.990	0.510	0.533	69.029	1.057	0.776	30.944	0.174	0.252	112.286
	48	0.361	0.354	41.951	0.330	0.400	36.132	0.570	0.577	40.947	1.019	0.765	17.091	0.189	0.261	59.510
	96	0.362	0.354	51.430	0.336	0.403	43.938	0.569	0.574	43.910	1.023	0.766	13.353	0.196	0.265	58.008
	192	0.361	0.354	58.848	0.341	0.407	53.038	0.574	0.573	71.913	1.015	0.763	10.608	0.208	0.271	50.885
	336	0.360	0.353	69.981	0.341	0.407	62.130	0.588	0.584	70.197	1.016	0.762	11.105	0.210	0.271	49.687
	720	0.360	0.353	63.802	0.341	0.407	62.789	0.589	0.585	69.971	1.018	0.761	11.730	0.216	0.276	56.289
CHBike	24	0.586	0.236	11.287	0.719	0.259	15.736	0.483	0.253	20.722	1.033	0.427	13.046	0.348	0.172	17.738
	48	0.598	0.238	54.795	0.720	0.258	49.071	0.528	0.263	23.159	1.044	0.429	7.855	0.350	0.177	18.073
	96	0.600	0.238	40.558	0.720	0.258	39.272	0.533	0.261	62.846	1.026	0.426	14.586	0.349	0.176	45.471
	192	0.597	0.237	54.833	0.721	0.259	53.351	0.536	0.263	76.555	1.016	0.423	15.592	0.347	0.175	57.547
	336	0.597	0.236	72.382	0.722	0.259	60.742	0.538	0.265	98.041	1.011	0.421	13.229	0.344	0.174	61.071
	720	0.600	0.237	110.547	0.723	0.259	89.368	0.538	0.264	136.728	1.006	0.416	17.090	0.361	0.187	86.629

Table 9: Full results of short/long-term forecasting comparing with baselines (2/2). The best scores are in **boldface**. The dataset names are abbreviated for briefness. "%" denotes the results are scaled by 1/100.

System		NDCN			GNS			ST-GODE			MT-GODE			PDEDER		
		MSE	MAE	MRAE	MSE	MAE	MRAE	MSE	MAE	MRAE	MSE	MAE	MRAE	MSE	MAE	MRAE
TDrive	24	0.292	0.283	15736.0	0.225	0.266	7574.2	0.431	0.446	27129.3	0.814	0.595	10453.3	0.116	0.168	15286.5
	48	0.311	0.297	16404.9	0.250	0.283	12647.7	0.491	0.471	30402.6	0.841	0.615	9791.7	0.121	0.169	16292.3
	96	0.328	0.309	16976.4	0.269	0.296	15117.7	0.483	0.461	28853.0	0.858	0.622	10139.2	0.132	0.175	17015.3
	192	0.345	0.318	18483.8	0.284	0.306	14503.9	0.494	0.463	26906.7	0.880	0.635	8501.7	0.142	0.180	16026.1
	336	0.373	0.333	18978.9	0.309	0.324	14032.6	0.530	0.473	23672.2	0.905	0.651	6640.1	0.163	0.194	14970.5
	720	0.421	0.367	19281.9	0.350	0.352	13592.2	0.574	0.476	17588.1	0.947	0.675	4550.2	0.205	0.226	14584.5
PEMS03	24	0.148	0.254	2.772	0.969	0.803	8.454	0.199	0.309	6.150	0.980	0.814	2.181	0.158	0.261	3.235
	48	0.198	0.297	6.223	1.022	0.826	7.937	0.200	0.311	7.615	1.016	0.835	3.276	0.213	0.306	5.120
	96	0.264	0.352	5.665	1.088	0.856	7.184	0.203	0.315	6.767	1.005	0.833	2.787	0.283	0.361	6.089
	192	0.317	0.395	6.167	1.141	0.881	7.096	0.206	0.319	6.655	1.014	0.839	3.075	0.328	0.398	8.279
	336	0.298	0.381	5.582	1.120	0.871	6.993	0.205	0.317	7.959	1.022	0.843	2.689	0.287	0.366	7.562
	720	0.335	0.411	5.651	1.138	0.879	8.358	0.205	0.317	7.027	1.024	0.844	2.469	0.311	0.389	7.290
PEMS04	24	0.465	0.396	6.577	1.032	0.689	4.049	0.534	0.526	4.554	0.980	0.694	2.481	0.663	0.488	4.007
	48	0.545	0.443	8.405	1.029	0.688	3.813	0.466	0.493	6.532	0.986	0.699	2.563	0.719	0.521	5.163
	96	0.655	0.504	11.508	1.027	0.687	4.201	0.408	0.462	5.515	0.994	0.704	2.444	0.803	0.568	6.158
	192	0.751	0.557	12.697	1.026	0.687	4.092	0.393	0.455	5.551	1.003	0.708	2.384	0.874	0.607	6.079
	336	0.741	0.547	14.319	1.026	0.687	4.168	0.394	0.456	5.520	1.008	0.710	2.596	0.829	0.581	5.964
	720	0.822	0.584	17.939	1.026	0.687	4.317	0.382	0.450	5.688	1.008	0.710	2.508	0.840	0.586	5.916
PEMS07	24	0.579	0.536	6.308	1.104	0.826	4.080	0.717	0.627	3.342	0.987	0.766	1.575	0.226	0.318	4.472
	48	0.578	0.535	6.438	1.098	0.824	4.099	0.716	0.627	3.320	0.989	0.772	1.551	0.300	0.370	5.353
	96	0.574	0.532	7.255	1.092	0.821	4.455	0.715	0.627	3.070	1.000	0.779	1.663	0.402	0.439	6.687
	192	0.574	0.533	7.332	1.090	0.820	4.471	0.715	0.627	3.439	1.002	0.781	1.796	0.479	0.493	6.500
	336	0.576	0.533	7.349	1.089	0.819	4.663	0.714	0.626	3.359	0.999	0.781	1.817	0.418	0.454	5.771
	720	0.575	0.533	7.609	1.088	0.819	4.788	0.714	0.626	3.259	1.000	0.782	1.767	0.439	0.472	6.644
PEMS08	24	1.009	0.628	8.452	0.933	0.688	2.788	0.853	0.751	3.725	1.024	0.718	3.145	0.623	0.476	8.177
	48	1.011	0.628	10.270	0.934	0.688	3.150	0.845	0.748	3.553	1.018	0.717	2.839	0.663	0.503	7.441
	96	1.011	0.628	11.651	0.935	0.688	3.638	0.862	0.753	4.006	1.009	0.715	2.619	0.729	0.544	7.716
	192	1.004	0.625	14.057	0.935	0.688	3.887	0.879	0.759	4.162	1.004	0.714	2.768	0.791	0.582	8.775
	336	1.003	0.624	13.029	0.935	0.688	3.784	0.872	0.756	4.040	1.008	0.715	2.721	0.768	0.569	8.102
	720	1.007	0.625	12.479	0.935	0.687	3.977	0.876	0.758	4.507	1.012	0.716	3.111	0.765	0.567	8.050
NOAA	24	0.485	0.510	8.817	0.567	0.560	17.798	0.578	0.568	3.129	0.952	0.708	5.074	0.324	0.408	17.031
	48	0.521	0.532	13.585	0.603	0.580	20.415	0.592	0.575	2.682	0.962	0.717	6.263	0.399	0.456	21.904
	96	0.622	0.584	15.519	0.700	0.626	22.065	0.648	0.604	2.853	0.990	0.730	5.623	0.533	0.524	26.829
	192	0.828	0.677	15.616	0.900	0.710	21.805	0.727	0.643	4.433	1.005	0.739	6.472	0.684	0.597	24.321
	336	0.840	0.681	14.823	0.914	0.715	21.309	0.738	0.649	3.735	1.014	0.745	6.714	0.742	0.629	22.113
	720	0.839	0.677	13.466	0.907	0.711	21.129	0.738	0.648	3.760	1.020	0.751	6.312	0.835	0.678	16.534

Table 10: Full results of short/long-term forecasting on variants of PDEDER (1/2). The best scores are in **boldface**. The dataset names are abbreviated for briefness. "%" denotes the results are scaled by 1/100.

System		PDEDER			PDEDER-nopre			PDEDER-frz			PDEDER-sys		
		MSE	MAE	MRAE	MSE	MAE	MRAE	MSE	MAE	MRAE	MSE	MAE	MRAE
Mutualistic	10%	0.276	0.386	5.702	0.420	0.516	6.379	0.213	0.356	5.949	0.298	0.415	6.136
	20%	0.448	0.518	5.820	0.642	0.669	6.491	0.414	0.504	6.075	0.491	0.562	6.208
	50%	0.750	0.656	3.675	0.971	0.805	4.140	0.774	0.678	3.896	0.840	0.718	3.947
	70%	0.813	0.679	2.879	1.008	0.819	3.256	0.827	0.698	3.040	0.915	0.745	3.097
	80%	0.829	0.683	2.625	1.014	0.817	2.972	0.836	0.698	2.762	0.931	0.747	2.824
	100%	0.844	0.683	2.259	1.020	0.808	2.564	0.835	0.687	2.359	0.939	0.742	2.430
Heat	10%	0.003	0.045	0.307	0.027	0.135	0.910	0.008	0.068	0.782	0.009	0.078	0.639
	20%	0.003	0.045	0.264	0.027	0.136	0.825	0.007	0.067	0.667	0.009	0.078	0.593
	50%	0.004	0.048	0.885	0.030	0.136	3.643	0.008	0.064	1.438	0.009	0.079	1.298
	70%	0.005	0.051	3.719	0.031	0.136	12.385	0.009	0.067	3.055	0.010	0.079	3.448
	80%	0.006	0.052	4.536	0.032	0.137	13.063	0.010	0.072	3.975	0.010	0.079	4.136
	100%	0.009	0.059	6.581	0.037	0.142	14.490	0.015	0.086	7.144	0.012	0.082	6.230
2D CFD	10%	0.230	0.309	1.158	0.231	0.309	1.170	0.232	0.317	1.196	0.229	0.303	1.069
	20%	0.216	0.296	1.212	0.217	0.296	1.221	0.218	0.304	1.249	0.215	0.291	1.122
	50%	0.177	0.261	1.539	0.179	0.261	1.704	0.180	0.270	1.734	0.176	0.256	1.389
	70%	0.155	0.240	1.715	0.158	0.241	1.878	0.158	0.249	1.872	0.154	0.236	1.590
	80%	0.146	0.230	1.861	0.149	0.231	2.044	0.149	0.239	2.003	0.145	0.226	1.731
	100%	0.130	0.212	2.118	0.119	0.205	2.325	0.133	0.221	2.248	0.129	0.209	1.993
DarcyFlow	10%	0.065%	1.998%	1.404	0.092%	2.338%	3.679	0.077%	2.140%	2.333	0.065%	2.002%	1.376
	20%	0.069%	2.034%	1.392	0.090%	2.307%	3.131	0.078%	2.154%	2.316	0.069%	2.044%	1.401
	50%	0.072%	2.063%	1.486	0.086%	2.256%	2.156	0.080%	2.176%	2.479	0.072%	2.079%	1.476
	70%	0.072%	2.065%	1.468	0.085%	2.236%	2.059	0.080%	2.180%	2.538	0.073%	2.086%	1.445
	80%	0.072%	2.065%	1.449	0.085%	2.231%	2.079	0.080%	2.181%	2.549	0.073%	2.088%	1.428
	100%	0.072%	2.065%	1.426	0.084%	2.224%	2.227	0.080%	2.180%	2.594	0.074%	2.092%	1.405
Gene	10%	0.033	0.135	1.528	0.138	0.309	1.790	0.101	0.224	2.342	0.051	0.183	1.652
	20%	0.036	0.138	1.499	0.141	0.312	1.704	0.124	0.248	2.409	0.053	0.185	1.590
	50%	0.052	0.152	1.796	0.151	0.319	1.817	0.219	0.344	3.461	0.058	0.184	1.784
	70%	0.069	0.167	1.928	0.159	0.320	1.873	0.303	0.414	3.963	0.066	0.188	1.891
	80%	0.079	0.176	1.985	0.163	0.320	1.894	0.348	0.447	4.092	0.073	0.193	1.928
	100%	0.103	0.194	2.268	0.177	0.324	2.066	0.438	0.508	4.638	0.089	0.204	2.243
ShallowWater	10%	0.582	0.327	1.611	0.994	0.415	0.732	0.713	0.356	0.923	0.733	0.353	0.965
	20%	0.766	0.389	2.183	1.006	0.418	1.450	0.794	0.385	1.565	0.813	0.382	1.643
	50%	1.085	0.500	1.930	1.044	0.434	1.071	0.985	0.458	1.406	0.985	0.445	1.406
	70%	1.152	0.529	1.938	1.057	0.438	1.065	1.036	0.480	1.421	1.033	0.466	1.409
	80%	1.165	0.536	1.866	1.061	0.439	1.038	1.050	0.485	1.380	1.047	0.471	1.364
	100%	1.179	0.543	2.106	1.066	0.440	1.315	1.066	0.490	1.620	1.063	0.475	1.612
2D DiffReac	10%	0.945	0.715	4.918	0.986	0.737	5.565	0.959	0.728	4.877	0.964	0.721	5.508
	20%	0.975	0.731	4.965	0.976	0.738	4.966	0.957	0.732	4.391	0.981	0.733	5.028
	50%	1.061	0.789	4.292	0.993	0.765	3.619	1.000	0.769	3.440	1.034	0.780	3.964
	70%	1.053	0.792	4.123	1.004	0.776	3.628	1.006	0.777	3.468	1.030	0.785	3.819
	80%	1.055	0.795	3.984	1.009	0.780	3.463	1.010	0.780	3.355	1.032	0.788	3.659
	100%	1.061	0.800	3.751	1.016	0.786	3.381	1.021	0.787	3.224	1.041	0.793	3.548
LA	10%	0.581	0.516	2.405	0.590	0.519	2.787	0.580	0.514	2.390	0.585	0.516	2.503
	20%	0.582	0.516	2.245	0.590	0.519	2.655	0.580	0.514	2.240	0.584	0.515	2.358
	50%	0.575	0.512	2.087	0.581	0.515	2.456	0.574	0.510	2.098	0.576	0.511	2.191
	70%	0.572	0.510	2.039	0.577	0.513	2.380	0.571	0.509	2.046	0.572	0.508	2.134
	80%	0.570	0.509	2.019	0.575	0.511	2.340	0.570	0.508	2.027	0.571	0.507	2.103
	100%	0.568	0.508	1.988	0.572	0.510	2.293	0.567	0.507	1.990	0.567	0.505	2.067
SD	10%	0.634	0.472	2.958	0.663	0.498	3.099	0.641	0.479	3.018	0.642	0.479	3.029
	20%	0.634	0.473	4.927	0.668	0.502	5.086	0.642	0.481	4.996	0.641	0.479	4.941
	50%	0.639	0.478	4.018	0.672	0.507	4.023	0.648	0.486	4.043	0.646	0.484	4.016
	70%	0.642	0.481	3.749	0.675	0.509	3.723	0.652	0.489	3.780	0.648	0.486	3.723
	80%	0.643	0.483	3.677	0.676	0.511	3.623	0.653	0.491	3.712	0.649	0.488	3.643
	100%	0.644	0.484	3.613	0.675	0.511	3.562	0.654	0.492	3.683	0.649	0.489	3.581

Table 11: Full results of short/long-term forecasting on variants of PDEDER (2/2). The best scores are in **boldface**. The dataset names are abbreviated for briefness. "%" denotes the results are scaled by 1/100.

System		PDEDER			PDEDER-nopre			PDEDER-frz			PDEDER-sys		
		MSE	MAE	MRAE	MSE	MAE	MRAE	MSE	MAE	MRAE	MSE	MAE	MRAE
NYCTaxi	24	0.174	0.252	112.286	0.179	0.257	113.806	0.211	0.300	83.433	0.185	0.263	114.767
	48	0.189	0.261	59.510	0.197	0.273	60.461	0.212	0.293	44.679	0.198	0.269	60.569
	96	0.196	0.265	58.008	0.211	0.281	60.900	0.214	0.284	47.414	0.206	0.272	57.876
	192	0.208	0.271	50.885	0.216	0.282	53.787	0.223	0.285	44.304	0.216	0.278	50.721
	336	0.210	0.271	49.687	0.213	0.276	52.057	0.215	0.278	46.323	0.214	0.277	51.752
	720	0.216	0.276	56.289	0.235	0.297	56.623	0.243	0.296	52.163	0.233	0.288	58.768
CHBike	24	0.348	0.172	17.738	0.520	0.213	23.882	0.431	0.198	19.476	0.302	0.165	19.628
	48	0.350	0.177	18.073	0.501	0.211	23.543	0.402	0.190	18.030	0.315	0.170	19.136
	96	0.349	0.176	45.471	0.466	0.204	52.778	0.384	0.183	43.365	0.322	0.172	42.505
	192	0.347	0.175	57.547	0.426	0.195	67.644	0.382	0.181	56.502	0.329	0.174	53.260
	336	0.344	0.174	61.071	0.394	0.187	69.650	0.374	0.179	60.060	0.332	0.174	56.850
	720	0.361	0.187	86.629	0.369	0.180	114.281	0.411	0.198	84.584	0.348	0.181	97.035
TDrive	24	0.116	0.168	15286.5	0.164	0.211	19079.9	0.154	0.197	14473.9	0.116	0.170	15618.7
	48	0.121	0.169	16292.3	0.167	0.216	20283.7	0.150	0.191	15643.0	0.121	0.171	16655.2
	96	0.132	0.175	17015.3	0.168	0.219	20387.7	0.152	0.192	16497.6	0.131	0.176	17389.7
	192	0.142	0.180	16026.1	0.170	0.219	18704.0	0.157	0.198	15550.5	0.142	0.182	16384.3
	336	0.163	0.194	14970.5	0.186	0.225	17032.2	0.174	0.212	14556.4	0.164	0.198	15269.7
	720	0.205	0.226	14584.5	0.220	0.246	16234.7	0.216	0.242	14261.4	0.207	0.230	14959.7
PEMS03	24	0.158	0.261	3.235	0.170	0.287	3.684	0.157	0.273	3.441	0.158	0.264	3.560
	48	0.213	0.306	5.120	0.233	0.335	5.774	0.215	0.317	5.535	0.218	0.312	5.698
	96	0.283	0.361	6.089	0.313	0.393	6.842	0.287	0.369	6.283	0.289	0.367	6.698
	192	0.328	0.398	8.279	0.367	0.432	9.395	0.331	0.403	8.364	0.333	0.403	8.922
	336	0.287	0.366	7.562	0.321	0.399	8.728	0.288	0.369	7.494	0.287	0.369	8.140
	720	0.311	0.389	7.290	0.330	0.406	8.446	0.301	0.385	7.427	0.321	0.398	7.726
PEMS04	24	0.663	0.488	4.007	0.671	0.502	4.484	0.649	0.482	3.975	0.652	0.479	3.946
	48	0.719	0.521	5.163	0.734	0.537	5.758	0.708	0.517	5.173	0.710	0.515	5.165
	96	0.803	0.568	6.158	0.834	0.590	6.948	0.798	0.568	6.221	0.797	0.565	6.177
	192	0.874	0.607	6.079	0.921	0.634	6.871	0.876	0.610	6.235	0.869	0.605	6.113
	336	0.829	0.581	5.964	0.868	0.605	6.748	0.830	0.582	6.105	0.825	0.579	6.034
	720	0.840	0.586	5.916	0.876	0.606	6.630	0.838	0.586	5.899	0.836	0.585	6.094
PEMS07	24	0.226	0.318	4.472	0.256	0.356	5.075	0.194	0.294	4.553	0.190	0.291	4.123
	48	0.300	0.370	5.353	0.348	0.417	6.265	0.281	0.358	5.601	0.277	0.356	5.205
	96	0.402	0.439	6.687	0.469	0.491	7.996	0.394	0.436	7.013	0.391	0.435	6.815
	192	0.479	0.493	6.500	0.556	0.546	7.721	0.472	0.491	6.764	0.476	0.494	6.721
	336	0.418	0.454	5.771	0.480	0.498	6.809	0.413	0.452	5.993	0.417	0.455	6.063
	720	0.439	0.472	6.644	0.473	0.499	7.525	0.425	0.465	6.416	0.439	0.474	7.261
PEMS08	24	0.623	0.476	8.177	0.642	0.509	9.626	0.621	0.476	8.323	0.617	0.475	8.631
	48	0.663	0.503	7.441	0.697	0.541	8.647	0.660	0.502	7.589	0.661	0.504	7.731
	96	0.729	0.544	7.716	0.786	0.588	9.096	0.727	0.544	7.804	0.729	0.547	7.954
	192	0.791	0.582	8.775	0.867	0.630	10.622	0.788	0.580	8.884	0.789	0.583	8.975
	336	0.768	0.569	8.102	0.831	0.610	9.663	0.764	0.567	8.191	0.764	0.569	8.254
	720	0.765	0.567	8.050	0.812	0.600	9.084	0.758	0.565	8.109	0.763	0.566	8.036
NOAA	24	0.324	0.408	17.031	0.331	0.415	15.150	0.375	0.444	19.176	0.336	0.418	17.995
	48	0.399	0.456	21.904	0.385	0.447	17.113	0.429	0.469	21.112	0.409	0.462	22.900
	96	0.533	0.524	26.829	0.499	0.509	22.450	0.542	0.525	23.307	0.554	0.533	27.712
	192	0.684	0.597	24.321	0.633	0.579	20.795	0.690	0.597	22.598	0.697	0.600	24.067
	336	0.742	0.629	22.113	0.692	0.610	17.663	0.774	0.639	20.318	0.749	0.626	21.997
	720	0.835	0.678	16.534	0.815	0.671	13.298	0.876	0.698	17.635	0.829	0.669	15.774

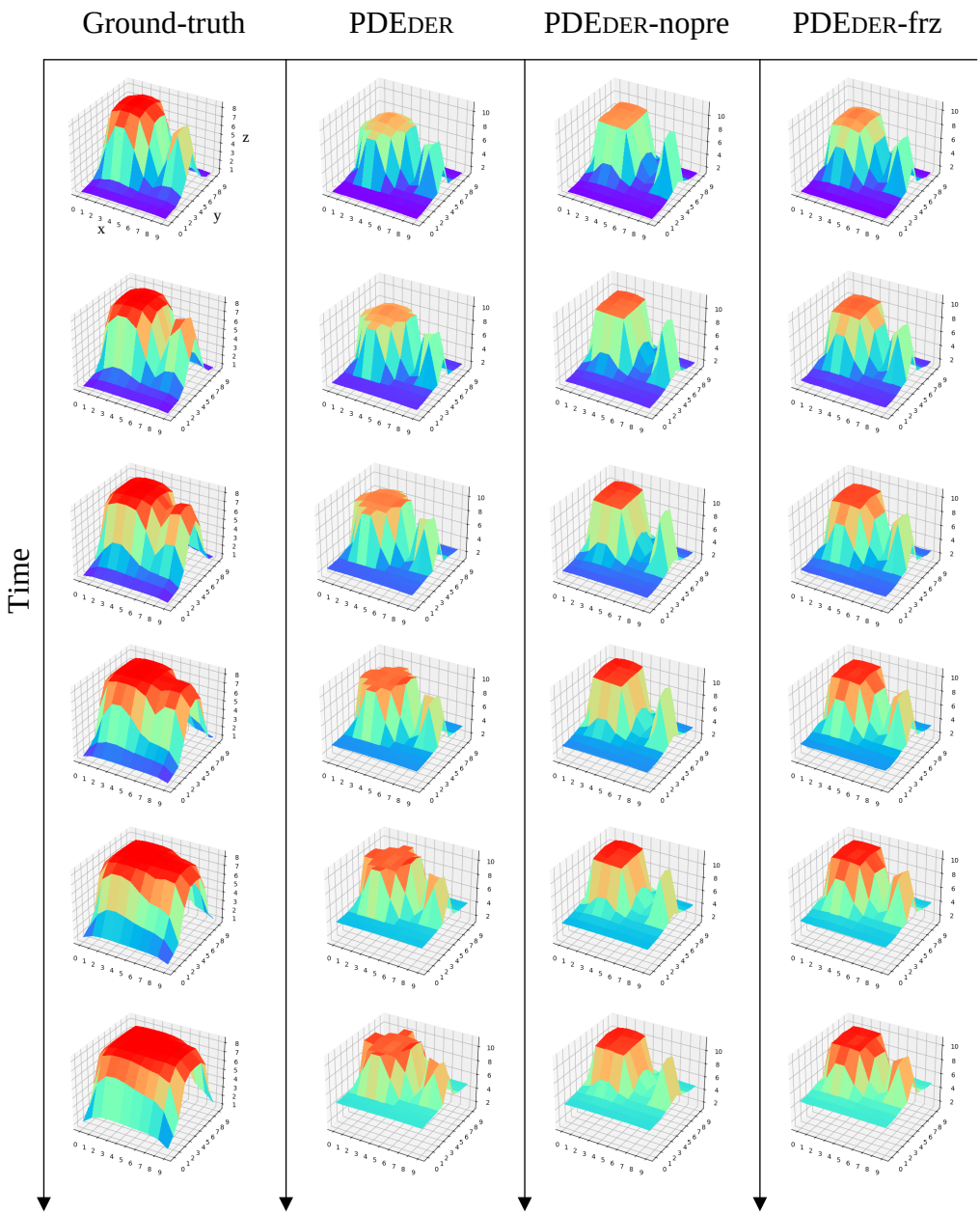

Figure 2: Forecasting visualizations on Mutualistic dynamics evolving comparisons between the ground-truth values, fine-tuning PDEDER, fine-tuning without pre-training PDEDER and fine-tuning with freezing the pre-trained PDEDER. Axes "x" and "y" denote the indexes of each object; axis "z" denotes the state values of each object.

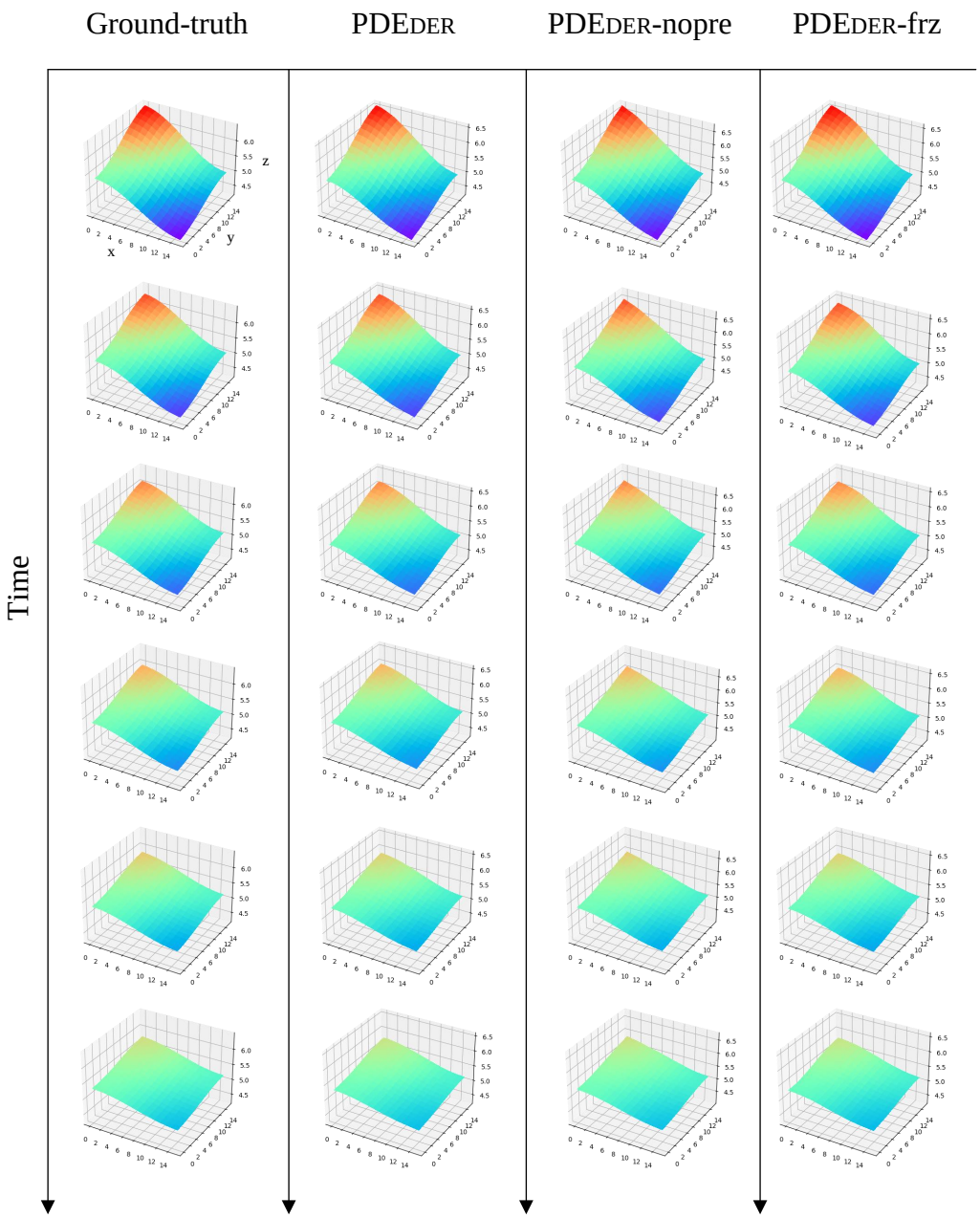

Figure 3: Forecasting visualizations on Heat dynamics evolving comparisons between the ground-truth values, fine-tuning PDEDER, fine-tuning without pre-training PDEDER and fine-tuning with freezing the pre-trained PDEDER. Axes "x" and "y" denote the indexes of each object; axis "z" denotes the state values of each object.

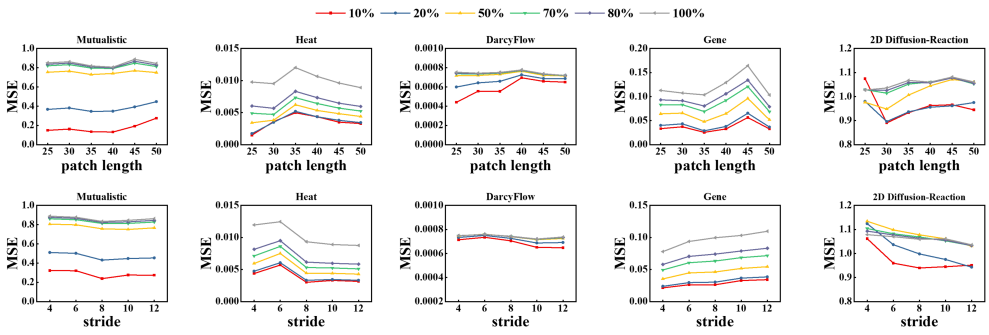

Figure 4: Sensitivity study results MSE on patch length and stride during fine-tuning PDEDER.